powder 2 power

MW-scale fluidized particle-driven CSP prototype demonstration

Grant Agreement n° 101122347

Definition of KPIs and methodology for techno-economic assessment

Deliverable 5.3

WP5 – Environmental, Social, Economic and Technical Performance Assessment

Due date of delivery:	31/03/2025	**Leading institution:**	KTH Royal Institute of Technology
Actual delivery date:	31/03/2025	**Contributor(s):**	Salvatore Guccione
			Rafael Guedez

Funded by the European Union

This project has received funding from the European Union's Horizon Europe research and innovation programme under the grant agreement No 101122347.

Deliverable Information

Deliverable Identification	POWDER2POWER_WP5_D5.3	
Deliverable title	Definition of KPIs and methodology for techno-economic assessment	
Related WP(s)	WP5 – Environmental, Social, Economic and Technical Performance Assessment	
Responsible Beneficiary	KTH – Royal Institute of Technology	
Author(s)	KTH	Salvatore GUCCIONE, and Rafael GUEDEZ
Reviewer(s)	EDF. POLIMI, B2Z, CNRS	Bo LIU, Frederic SIROS, Benjain CASTELNAU (EDF) Marco BINOTTI (POLIMI) Mariola GUERRERO GARRIDO (B2Z) Sergio MARIN ZAPATA, Gilles FLAMANT (CNRS)
Due delivery date	31/03/2025	
Actual delivery date	31/03/2025	
Version - Date	V1.0 – 31/03/2025	
Summary	This deliverable defines the upscaled layout of the Powder2Power project and introduces the techno-economic modeling approach, including thermodynamic models and cost functions. MoSES, a modeling tool developed in Task 5.3, supports simulation activities for evaluating project benefits. A comprehensive KPI panel, categorized into technical, economic, environmental, and mixed indicators, is integrated into MoSES for system optimization. The report details the modeling approach, key equations, and customizable inputs for system design and performance analysis. Future activities will focus on model development, verification, and incorporating partner feedback.	
Deliverable type	R – Report	
Dissemination level	PU - Public	
Repository	*Intranet, Website*	

Document History and Approval

Version	Date	Action	Name & Organization
V0.1	12/02/2025	Full Draft shared	Salvatore GUCCIONE and Rafael GUEDEZ (KTH)
V0.2	19/03/2025	Revised version based on feedback from EDF; POLIMI, and B2Z	Salvatore GUCCIONE (KTH)
V0.3	25/03/2025	Revised version based on feedback from EDF; POLIMI, and B2Z	Salvatore GUCCIONE (KTH)
V0.4	26/03/2025	Revised version based on feedback from CNRS	Salvatore GUCCIONE (KTH)
V1.0	31/03/2025	Final version	Sergio MARIN ZAPATA (CNRS)

Acknowledgment and legal disclaimer

This report is part of the project that has received funding from the European Union's Horizon Europe research and innovation programme under the grant agreement No 101122347. The content of this publication is the sole responsibility of the POWDER2POWER project.

POWDER2POWER Project Factsheet

Grant Agreement n°	101122347	Project Acronym	POWDER2POWER
Project Full Title	MW-scale fluidized particle-driven CSP prototype demonstration		
Call identifier	HORIZON-CL5-2022-D3-03 "Innovative components and/or sub-systems for CSP plants and/or concentrating solar thermal installations"		
Funding instrument	Innovation Action		
Project start date	01/09/2023	Duration	48 months
Website	www.powder2power-project.eu		
Partners Short Name	• PROMES-CNRS • EDF • EPPT • JCR • B2Z • POLIMI • KTH • CSPB • SEI • KUL		

WP	Task
WP1 - Project Management (CNRS)	Task 1.1 – Administrative, legal, and financial management
	Task 1.2 – Quality Management
	Task 1.3 – Coordination of the activities
	Task 1.4 – Data Management Plan
WP2 - Particle Behavior, Transport and Handling (EPPT)	Task 2.1 – Particle flow properties as a function of temperature
	Task 2.2 – Erosion, attrition and dust emission
	Task 2.3 – Assessment of particle transport issues at pilot & commercial scale
	Task 2.4 – Design & construction of the particle conveyance system for the P2P pilot plant
	Task 2.5 – Design & construction of the particle electrical heater
WP3 - Solar Pilot Modification, Component testing and complete Pilot Demonstration (CNRS)	Task 3.1 – Pilot loop modification and implementation
	Task 3.2 – Commissioning of the particle loop
	Task 3.3 – Complete solar pilot testing
	Task 3.4 – Guideline for operation and maintenance
WP4 - P2P Technology Up-scale Towards Commercialization (B2Z)	Task 4.1 – Definition of up-scaled integrated P2P power plant layouts, including PV + heaters hybridization
	Task 4.2 – Design of a utility-scale heliostat field and solar receiver
	Task 4.3 – Design of a utility-scale particle-to-sCO_2 heat exchanger
	Task 4.4 – Design of utility-scale electrical heating system
	Task 4.5 – Design of utility-scale sCO_2 cycle
WP5 - Environmental, Social, Economic and Technical Performance Assessment (EDF)	Task 5.1 – Definition of optimal operational strategies and flexibility assessment of the utility scale P2P plant
	Task 5.2 – Techno-economic assessment of a utility-scale hybrid CSP-PV P2P power plant
	Task 5.3 – Techno-economic model development & verification
	Task 5.4 – Environmental and social impact assessment via LCA and sLCA modelling
	Task 5.5 – Social impact assessment of the best identified cases
WP6 - Communication, Exploitation, Dissemination (CSPB)	Task 6.1 – Identification and protection of exploitable results
	Task 6.2 – Exploitation and dissemination of the project results
	Task 6.3 – Communication activities results

Executive summary

This report presents the upscaled layout of the Powder2Power project, detailing the techno-economic modeling approach, including thermodynamic models of components and bottom-up cost functions. The report introduces MoSES (Modeling of Solar Energy Systems) as a tool in Task 5.3, supporting the evaluation of Powder2Power benefits through simulation activities. MoSES facilitates the design, optimization, and benchmarking of various solar plant layouts. The report elaborates on the modeling approach for simulating and optimizing the performance of the hybrid solar system under investigation, emphasizing system design, cost structures, and expected performance metrics.

A comprehensive Key Performance Indicator (KPI) panel is defined to evaluate the project's benefits. KPIs are categorized into technical, economic, environmental, and mixed indicators. These KPIs monitor project benefits, target achievements, and the techno-economic viability of the Powder2Power plant. The KPI panel is integrated into MoSES, allowing users to select any KPI as an objective function during system optimization. The report also highlights the main equations used in thermodynamic and cost models, detailing customizable inputs and expected outputs for system design and operation. Future activities in Task 5.3 will focus on further model development, verification, and incorporating feedback from project partners and industrial stakeholders.

Table of Contents

List of Figures

List of Tables

List of Acronyms and Abbreviations

Acronym / Abbreviation	Meaning / Full text
AEY	Annual Energy Yield
AF	Availability Factor
CAPEX	Capital Expenditure
CF	Capacity Factor
CO	Carbon Monoxide
CO2	Carbon Dioxide
CSP	Concentrating Solar Power
CV	Capacity Value
DNI	Direct Normal Irradiance
DPB	Discounted Pay-Back Period
EC	European Commission
EPC	Engineering, Procurement and Construction
EU	European Union
EUR	Euro
FF	Flexibility Factor
FOAK	First-of-a-Kind
GHG	Greenhouse gas
HTF	Heat Transfer Fluid
KPI	Key Performance Indicator
LCOE	Levelized Cost of Electricity
LOLP	Loss-of-Load-Probability
NOx	Nitrogen Oxides
NPV	Net Present Value
OPEX	Operational Expenditure
PPA	Power Purchase Agreement
PV	Photo-Voltaic
RC	Ramping Capability
RES	Renewable Energy System
SC	Specific Cost
SDD	Shut-Down Duration
SET	Strategic Energy Technology
SLU	Specific Land Use
SOx	Sulphur Oxides

SUD	Start-Up Duration
SWC	Specific Water Consumption
TES	Thermal Energy Storage
TRL	Technology Readiness Level
UF	Utilization Factor
VALCOE	Value-Adjusted Levelized Cost of Electricity

1. Introduction

This document represents the Deliverable D5.3 "Definition of KPIs and methodology for techno-economic assessment", related to Task 5.3, within WP5.

1.1. Task Description

The aim of task T5.3 is to develop appropriate techno-economic models, valorizing previous modeling work carried out by KTH in sister EU projects by enhancing KTH's in-house tool (MoSES – Modeling of Sustainable Energy Systems) with new system layouts and correlations cross-validated with partners. The work will integrate operational maps developed in T5.1 for assessing the benefits of the proposed P2P system (from T4.1) and enable the use of this tool for comparison against standard and commercial CSP systems under user-defined assumptions. These models will account for the calculation of technical, economic, and environmental KPIs. The developed models will be used as a basis in T5.2 for a comprehensive performance assessment. This deliverable primarily focuses on developing bottom-up cost functions and defining KPIs for hybrid layouts. It involves identifying all relevant costs, including design, acquisition, installation, and maintenance. Cost functions for up-scaled systems will be created, incorporating uncertainty and sensitivity analyses to optimize the P2P system from both technical and economic perspectives. A selection of technical and financial KPIs related to construction, operation, maintenance, and decommissioning will be established and monitored throughout the techno-economic assessment. Additionally, relevant elements of optimization modeling will be integrated where necessary to support comprehensive system evaluation.

1.2. Report Structure

Section 1 provides a brief introduction to the Powder2Power (P2P) concept, including the task description and report structure. Section 2 presents a system description of an upscaled P2P concept, covering hybridization strategies that integrate solar photovoltaic (PV), battery energy storage systems (BESS), and electric heaters (EH). Section 3 outlines the techno-economic modeling approach, detailing the thermodynamic models used to characterize the system, as well as the cost functions and assumptions applied in the analysis. Section 4 introduces the key performance indicators (KPIs) used to benchmark and compare the different system configurations. These indicators are categorized into technical, economic, environmental, and mixed metrics, with each one defined and accompanied by its respective equation. Finally, Section 5 summarizes the key findings of the analysis and discusses future research directions planned for the P2P project.

1.3. Introduction to P2P concept

The Powder2Power (P2P) project addresses the urgent need for cost-effective, dispatchable renewable energy solutions to support the transition toward a sustainable and decarbonized global energy system. By developing an innovative concentrated solar power (CSP) technology with integrated thermal energy storage, P2P directly contributes to reducing reliance on fossil fuels and increasing the resilience of renewable energy supply. This project plays a pivotal role in enhancing the efficiency and affordability of solar power while ensuring its availability during periods of low solar radiation.P2P advances fluidized particle-driven CSP technology, building on previous research efforts and technological developments. By enabling the upscaling, implementation, and commercialization of this innovative solution, the project strengthens industrial competitiveness and supports the large-scale deployment of renewable energy in key markets. The technology's ability to provide high-temperature heat also creates new opportunities for decarbonizing industrial sectors, further broadening its impact. The primary objective of the P2P project is to develop and validate a high-efficiency CSP system that integrates advanced thermal energy storage, enabling the stable and reliable generation of solar power. The project focuses on improving efficiency, reducing costs, and demonstrating the technical feasibility of a particle-based CSP system capable of replacing conventional energy sources. A key innovation within P2P is the development of high-temperature fluidized bed heat exchangers that transfer thermal energy to a supercritical CO2 cycle, significantly enhancing overall efficiency. By addressing key technical challenges, such as thermal losses and operational flexibility, P2P aims to position CSP as a viable alternative for both electricity generation and industrial heat applications. Furthermore, the project fosters international collaboration, reinforcing scientific expertise and accelerating the path to commercialization. A fundamental aspect of the P2P project is the techno-economic analysis, which evaluates the financial and technical viability of the proposed CSP technology. This deliverable introduces the methodology used to assess efficiency, cost-effectiveness, and market potential. The analysis involves energy system modeling to simulate solar field and receiver efficiency using tools such as SolarPILOT and proprietary computational models. The integration of thermal energy storage is examined to determine its impact on dispatchability, while comparative assessments between molten salt and particle-driven CSP systems provide insights into performance improvements. A detailed cost analysis will estimate capital and operational expenditures for different configurations, alongside levelized cost of electricity calculations for various deployment scenarios. Sensitivity analyses will be conducted to assess the influence of critical cost drivers, such as storage duration and component efficiency. Performance evaluation focuses on quantifying efficiency gains enabled by operating at higher temperatures. The effectiveness of heat exchangers in transferring thermal energy from particles to supercritical CO2 is assessed, along with the startup and shutdown characteristics of the P2P system compared to molten salt-based CSP technologies. Additionally, market competitiveness and scalability will be examined to determine commercialization potential. This includes evaluating economic and regulatory factors, benchmarking against alternative renewable energy storage solutions, and analyzing the complementary role of P2P alongside photovoltaic and battery storage technologies. The techno-economic analysis will provide a comprehensive understanding of the financial and technical feasibility of P2P technology. The findings will highlight its potential to reduce costs, improve efficiency, offer cost-effective and long-duration energy storage solutions, and enhance the reliability of renewable energy integration in industrial applications. By applying this structured methodology, the P2P project aims to validate its technological advancements and support its transition toward commercial deployment, reinforcing its role as a key enabler of a sustainable energy future.

2. P2P System Description

The schematic of the upscaled particle-based hybrid PV-CSP plant analyzed in this project is shown in Figure 1. A conventional PV plant is hybridized with a central tower CSP system featuring a particle receiver, a direct two-tank thermal energy storage (TES) system, and a supercritical CO_2 (sCO_2) Brayton power block. The hybridization between PV and CSP is achieved by using an electric heater for particles. In Figure 1, the electric heater is integrated in series with the receiver, so the particles are first heated in the receiver and then their temperature is further boosted in the electric heater.

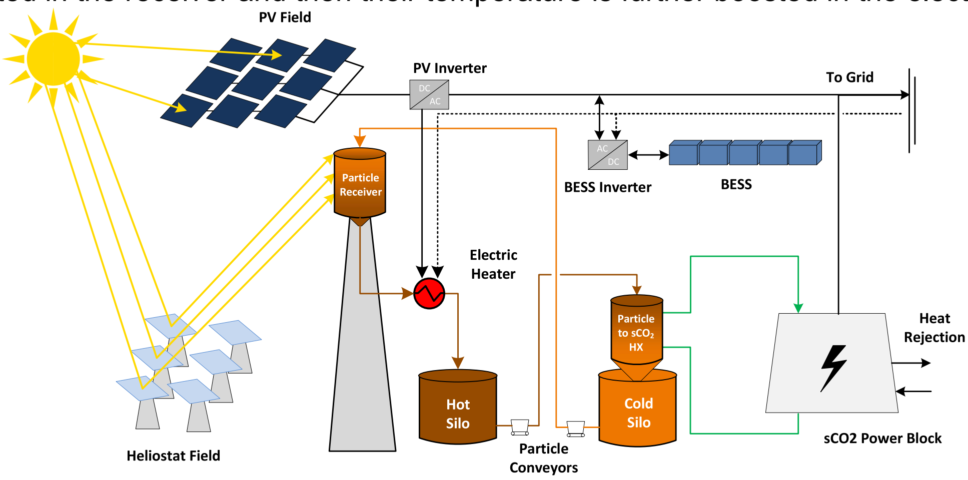

Figure 1. Layouts of the particle-based hybrid PV-CSP system with EH in series.

In the presence of a defined electricity market framework, the operation of the hybrid PV-CSP plant is governed by an operational dispatcher or a market-based control strategy. This dispatcher determines how and when the plant should operate—deciding, for instance, when the PV system should inject electricity into the grid, when to store energy either in the battery energy storage system (BESS) or in the thermal energy storage (TES) via the electric heater (EH), and when to purchase electricity from the grid to charge the TES. The plant's operation is always constrained by the requirement that, as soon as the solar field begins concentrating solar irradiance onto the receiver, sufficient electricity—either from the PV system or the grid—must be available to boost the particles' temperature to their design conditions in the TES. If no electricity market constraints are imposed, the plant is assumed to operate with the goal of maximizing total electricity production, optimizing internal energy flows accordingly.

The particle receiver is placed on top of the solar tower to convert the power collected by the heliostat field into thermal power. The particles are just partially heated into the receiver and then the temperature is boosted in the electric heater. Then, the particles are stored in a two-tank TES that decouples the sCO_2 power block electricity production from the intermittent solar-based heat production. During the discharge phase, the thermal-to-electric reconversion is realized by using a sCO_2 power block. For the power block, a sCO_2 power cycle is adopted. The sCO_2 power block is represented as a box in Figure 1. The sCO_2 Brayton cycle is a thermodynamic power cycle that employs CO_2 above its critical point (31 °C, 7.3 MPa) as the working fluid. Compared to traditional steam-based cycles, it offers the potential for higher thermal efficiency when operating at temperatures between 500 and 800 °C and pressures ranging from 20 to 30 MPa. Moreover, the sCO_2 Brayton cycle is characterized by compact and scalable pieces of equipment, which contribute to reduced capital costs, even at small scales. Increasing the temperature at the turbine inlet and introducing higher complexity into the cycle layout both contribute to increased efficiency and a higher return CO_2 temperature. Nevertheless, it is important to emphasize that these advancements also result in elevated system costs. To determine the suitability of sCO_2 power blocks for efficient and sustainable power generation applications, it is essential to conduct a comprehensive investigation into their properties and performance. In this study, four different power block configurations have been outlined modifying the simple recuperated sCO_2 Brayton cycle. Figure 2 shows the schematics of the different configurations of sCO_2 power blocks investigated in line with the results from WP4 and .

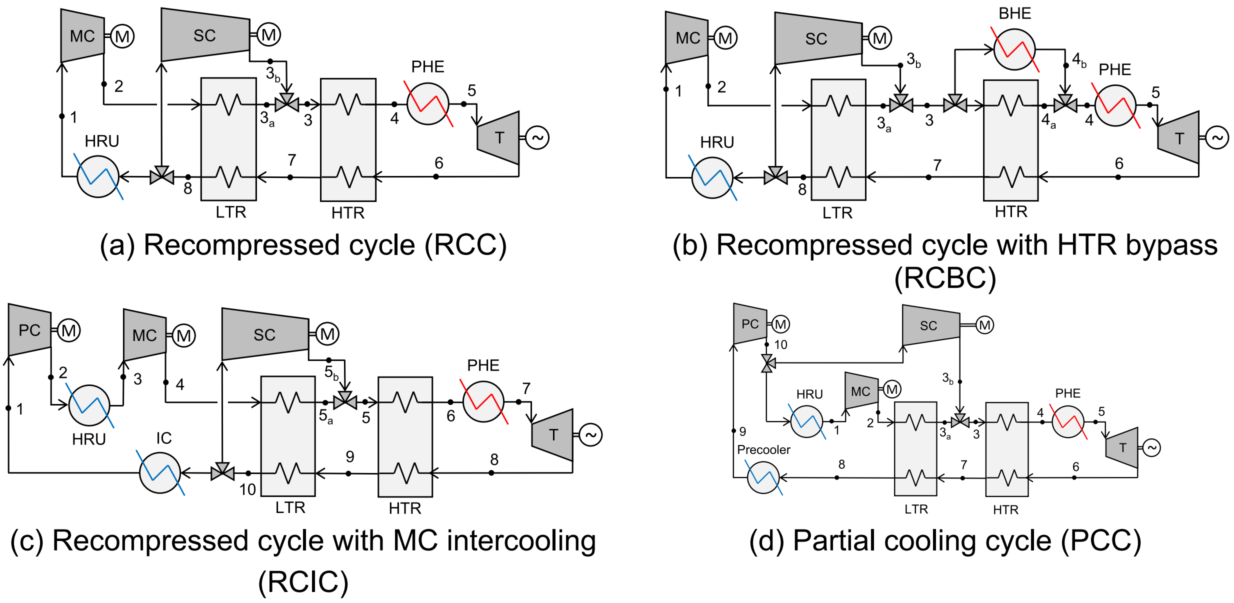

(a) Recompressed cycle (RCC)

(b) Recompressed cycle with HTR bypass (RCBC)

(c) Recompressed cycle with MC intercooling (RCIC)

(d) Partial cooling cycle (PCC)

Figure 2. sCO2 power block configurations investigated.

3. Techno-Economic Modeling Approach

This section presents the methodology used to assess the techno-economic performance of the particle-based hybrid PV-CSP system, highlighting the key modeling tools, the role of Key Performance Indicators (KPIs) in system optimization, and the main steps involved in plant design and optimization. The techno-economic analysis of the hybrid solar plant was conducted using a quasi-steady-state model developed in MoSES (Model of Sustainable Energy Systems). MoSES, developed at KTH Royal Institute of Technology, is a simulation tool designed for the pre-design, operation, and optimization of hybrid renewable energy systems with storage, including solar and wind technologies for both grid-connected and cogeneration industry applications.
For this project, MoSES was employed to estimate the techno-economic performance of hybrid CSP-PV power plants, incorporating various cost factors, design assumptions, and meteorological conditions [1], [2]. The tool integrates CoolProp [3] for thermophysical properties and the NREL-PySAM wrapper to interface with the System Advisor Model (SAM) [4]. MoSES features a comprehensive library of models, including both well-established subsystems and newly developed components, enabling a detailed and flexible evaluation of system performance.

The performance of state-of-the-art components has been validated through a comparison with SAM estimates. Furthermore, ad hoc models for components that are still undergoing development have been devised through a combination of literature review and collaboration with industrial partners and equipment manufacturers. These models have been verified against anticipated performance curves documented in existing literature. The techno-economic indicators have been evaluated by coupling thermodynamics with an economic model based on a bottom-up estimation method, as shown in Figure 3. The resulting system model is customizable in terms of location (meteorological data, grid availability, electricity market, and economics of location), design assumptions, and dispatch strategy.

The particle-based hybrid CSP-PV layout in this project will be designed through the resolution of a multi-objective optimization problem. Objective functions such as levelized cost of energy (LCOE), hybrid capacity factor (HCF), capital expenditure (CAPEX), annual energy yield (AEY), and maximum profit as well as the design variables can be customized by the users. To solve the optimization problem, a Genetic Algorithm is implemented, which utilizes principles of natural selection and genetics to obtain a set of tradeoff optimal solutions through evolutionary strategies [5]. The optimization problem has been implemented in Python using Pymoo [6]. The algorithm follows the general outline of NSGA-II with modified survival selection [7]. Dispatch optimization is implemented using Pyomo [8] to manage the system's decisions on when to store electricity, when to store heat, when to produce electricity, and when to purchase electricity. The optimal dispatch can be tailored to minimize energy waste, maximize revenues, and maximize CO_2 equivalent savings.

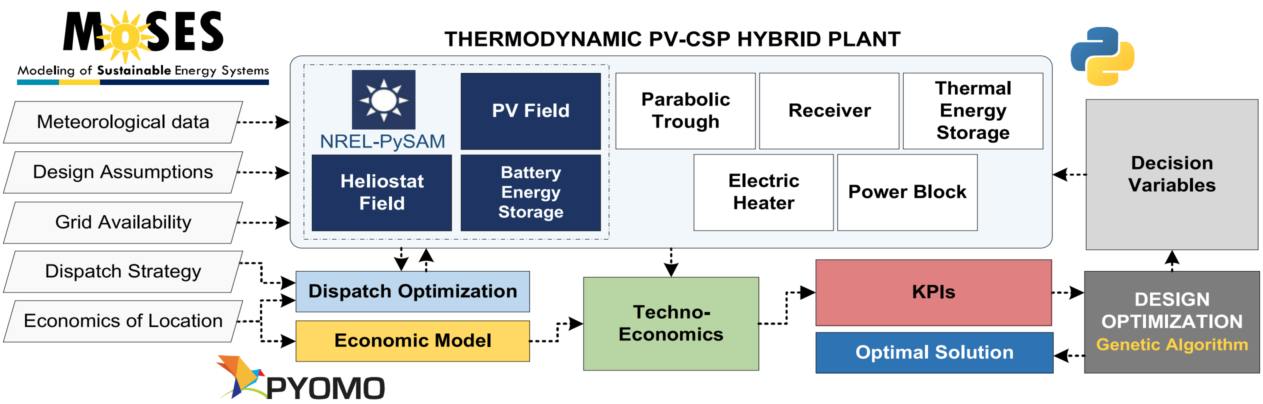

Figure 3. MoSES modeling methodology flowchart.

3.1. Thermodynamic models of the system

This section provides the main equations employed to build the quasi-static models of the different subsystems mentioned in section 2.

3.1.1. Sun

The weather file provided as the only input for the sun model is unpacked using the module weather file reader (*Wfreader*), included in the tool NREL-PySAM. Table 2 summarizes the model outputs, of which some are extracted from the weather file, while the rest such as the sun positions are estimated using the Duffie and Beckman algorithm [9].

Table 1. Operating Inputs – sun model

Symbol	Description	Unit
w_{file}	Weather file	[-]

Table 2. Operating Outputs – sun model

Symbol	Description	Unit
$time_s$	Timestep in seconds	[s]
hra_{deg}	Hour angle	[deg]
dec_{deg}	Declination angle	[deg]
ele_{deg}	Elevation angle	[deg]
azi_{deg}	Azimuth angle	[deg]
zen_{deg}	Zenith angle	[deg]
DNI	Direct Normal Irradiance	[W/m2]
GHI	Global Horizontal Irradiance	[W/m2]
DHI	Diffuse Horizontal Irradiance	[W/m2]
T_{amb}	Ambient temperature	[K]
W_{spd}	Wind speed	[m/s]
lon	Location longitude	[deg]
lat	Location latitude	[deg]
t_{zone}	Location time zone	[h]
$elev_{site}$	Elevation of the location	[m]

3.1.2. Heliostat Field

The heliostat field is designed and optimized for a specific site and target power output. The solar field design and optical performance map—used to estimate operating performance—can be derived by integrating performance maps provided by CSPB based on WP4's work. Alternatively, the main outputs of the model can be obtained using SolarPILOT, a module within the NREL-PySAM tool. The design process includes determining the optimal tower height and receiver area. For the selected solar field layout, an optical efficiency map is generated to assess the power concentrated on the receiver under varying irradiance conditions. When using external tubular receivers, a surrounding solar field is typically employed. However, because the particle system utilizes a cavity receiver, a single-sided solar field is required. This configuration addresses the receiver's thermal power constraints and prevents excessive thermal losses, thereby excluding the use of surrounding solar fields. When the heliostat field power exceeds a user-defined threshold (e.g., 150 MW), a multi-CSP tower configuration is adopted to manage the receiver's maximum thermal power and maintain relatively high optical efficiency. Finally, for a specified net power to be installed and a given SM input, the model calculates the number of CSP plants that must be installed in parallel to meet the required demand. Figure 4 (left) illustrates the heliostat field area for different solar field design powers, and in Figure 4 (right) shows the corresponding solar tower height and receiver aperture area for the same design power levels.

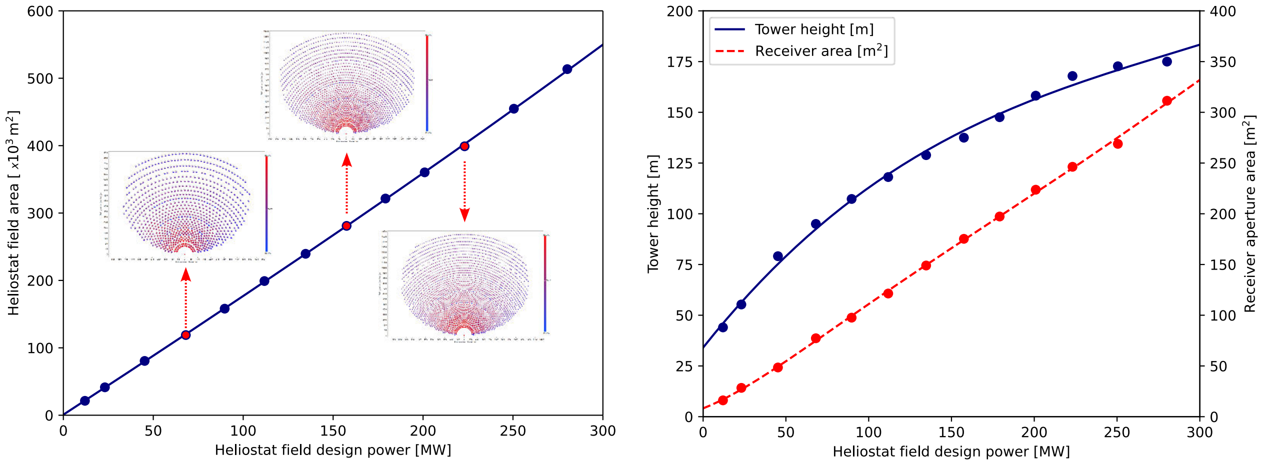

Figure 4. Heliostat field area (left) and tower height with receiver aperture area (right) as functions of the solar field design power.

Design

Table 3 summarizes the main inputs required for the heliostat field design. If the design is performed with SolarPILOT, the tool offers the possibility to optimize the solar field, the tower height, and the receiver dimensions based on a trade-off between the costs of these components and the performance of the solar field. The optimization is performed if the Boolean $Optimize_{SF}$ is true. In that case, the specified cost inputs are required. If the receiver is a flat plate receiver, further inputs are required. The design outputs are estimated as shown in the equations below and they are summarized in Table 4.

Table 3. Design Inputs - heliostat field model

Symbol	Description	Unit
DNI_{des}	Direct Normal Irradiance at the design point	[W/m2]
$helio_{width}$	Width of the heliostat	[m]
$helio_{height}$	Height of the heliostat	[m]
$excl_{fac}$	Exclusion factor (mirror density)	[-]
he,av_{design}	Heliostats availability	[-]
$H_{tower_{input}}$	Input of the tower height	[m]
$Q_{rec_{des}}$	Design receiver output power	[W]
$FlatPlate/\ Cavity$	Boolean to decide if the receiver is a Flat Plate/Cavity (Otherwise Surrounded Field)	[-]
$Optimize_{SF}$	Boolean to run optimization of the solar field	[-]
w_{file}	Weather file	[-]
c_{atm_0}	Attenuation coefficient 0	[-]
c_{atm_1}	Attenuation coefficient 1	[-]
c_{atm_2}	Attenuation coefficient 2	[-]
c_{atm_3}	Attenuation coefficient 3	[-]
$calc_{fluxmaps}$	Boolean to decide to include fluxmap calculations	[-]
$cant_{type}$	Heliostat cant method	[-]
$check_{max_{flux}}$	Boolean to decide to check max flux at design point	[-]
$delta_{flux_{hrs}}$	Hourly frequency in flux map lookup. If not provided	[-]
$flux\_max$	Maximum allowable flux. If not provided	[W/m2]
$focus_{type}$	Heliostat focus method	[-]

$helio_{optical_{error}}$	Optical error. If not provided	[rad]
$helio_{reflectance}$	Heliostats reflectance	[-]
$land_{max}$	Maximum land multiplier	[-]
$land_{min}$	Minimum land multiplier	[-]
n_facet_x	Number of heliostat facets - X	[-]
n_facet_y	Number of heliostat facets - Y	[-]
n_flux_days	Number of days in flux map lookup	[-]
n_flux_x	Flux map X resolution.	[-]
n_flux_y	Flux map Y resolution.	[-]
$fixed\_land\_area$	Plant area not occupied by the solar field.	[acre]
$opt\_algorithm$	Optimization algorithm.	[-]
opt_conv_tol	Optimization convergence tol.	[-]
$opt\_flux\_penalty$	Optimization flux overage penalty.	[-]
opt_init_step	Optimization initial step size.	[-]
opt_max_iter	Max. number iteration steps	[-]
$land\_overhead\_factor$	Land overhead factor	[-]
$rec\_absorptance$	Receiver coating absorptance	[-]
$rec\_hl\_perm\_guess$	Receiver design heat loss	[kW/m2]
	Inputs if $FlatPlate/Cavity\ = False$	
$D_{rec_{input}}$	Receiver diameter	[m]
$ar_{rec_{input}}$	Receiver aspect ratio (height/width)	[-]
	Inputs if $FlatPlate/Cavity\ = True$	
$W_{rec_{input}}$	Receiver width	[m]
$H_{rec_{input}}$	Receiver height	[m]
$span_{rec_{input}}$	Receiver span angle	[deg]
$n_{rec_{panels}}$	Number of receiver panels	[-]
	Inputs only if $Optimize_{SF} = True$	
$tower_{fixed_{cost}}$	Tower reference cost for cost function	[USD]
$tower_{exp}$	Exponent for tower cost function	[-]
$C_{receiver_{ref}}$	Receiver reference cost for cost function	[USD]
$A_{receiver_{ref}}$	Receiver reference area for cost function	[m2]
$rec_{cost_{exp}}$	Exponent for the receiver cost function	[-]
$site_{spec_{cost}}$	Site improvement specific cost	[USD/m2]
$heliostat_{spec_{cost}}$	Heliostat field specific cost	[USD/m2]
$cost_{sf_{fixed}}$	Heliostat field fixed cost	[USD]
$land_{spec_{cost}}$	Land specific cost	[USD/acre]
$contingency_{rate}$	Contingency rate	[%]
$sales_{tax_{frac}}$	Share of tax fraction	[%]
$sales_{tax_{rate}}$	Tax rate	[%]

$$A_{single_{heliostat}} = helio_{width} \cdot helio_{height} \quad (1)$$

$$D_{tower} = D_{rec} \quad (2)$$

$$C_{ratio} = \begin{cases} \dfrac{A_{SF}}{W_{rec} \cdot H_{rec}} & if\ FlatPlate/Cavity = True \\ \dfrac{A_{SF}}{\pi \cdot D_{rec} \cdot H_{rec}} & otherwise \end{cases} \quad (3)$$

Table 4. Design Outputs - heliostat field model

Symbol	Description	Unit
A_{SF}	Heliostat field area	[m2]
$n_{heliostat}$	Number of heliostats	[-]
$A_{single_{heliostat}}$	Area of single heliostat	[m2]
$A_{land_{base}}$	Base land area	[m2]
$A_{land_{tot}}$	Total land area	[m2]
H_{tower}	Tower height	[m]
H_{rec}	Receiver height	[m]
ar_{rec}	Receiver aspect ratio	[m]
D_{rec}/w_{rec}	Receiver diameter/width	[m]
D_{tower}	Tower diameter	[m]
C_{ratio}	Receiver concentration ratio	[m]
Map_{Helio}	Map of heliostat field	[-]
$SP_{SF_{Efficiency}}$	Heliostat field optical efficiency map	[-]

Operation

Table 5 summarizes the main hourly inputs required for the estimation of the operating performance of the heliostat field. The outputs are estimated by using the equations (4) –(15) and they are summarized in Table 6.

Table 5. Operation Inputs - heliostat field model

Symbol	Description	Unit
A_{SF}	Heliostat field area	[m2]
DNI	Hourly direct normal irradiance	[W/m2]
Q_{design}	Heliostat field design power	[W]
$Q_{defocus}$	Heliostat field defocus power	[W]
$Q_{loss_{rec_{des}}}$	Receiver thermal losses at the design point	[W]
nu_{start}	Minimum energy start-up fraction to start the receiver	[-]
nu_{min}	Minimum turn-down energy fraction to stop the receiver	[-]
ele	Elevation angle	[rad]
ele_{min}	Heliostat stow deploy angle	[rad]
w_{spd}	Wind speed	[m/s]
$w_{spd_{max}}$	Wind stow speed	[m/s]
$defocus$	Boolean to indicate if defocus	[-]
$SF_{on_{prev}}$	Previous boolean value to indicate if SF was on	[-]
$eff_{field_{SP}}$	Optical efficiency from SolarPILOT	[-]
hra	Hour angle	[rad]
dec	Declination angle	[rad]
$n_{heliostat}$	Number of heliostats	[-]
W_{track}	Tracking power for a single heliostat	[W]
he_{av}	Heliostats availability	[-]

$$Q_{in_{SF}} = A_{SF} \cdot DNI \tag{4}$$

$$eta_{field} = f(hra, dec) \tag{5}$$

$$Q_{raw} = \begin{cases} Q_{in_{SF}} \cdot eta_{field} & if\ ele > ele_{min}\ and\ w_{spd} < w_{spd_{max}} \\ 0 & otherwise \end{cases} \tag{6}$$

$$Q_{start} = nu_{start} \cdot Q_{design} \tag{7}$$

$$Q_{min} = nu_{min} \cdot Q_{design} \tag{8}$$

$$SF_{on} = \begin{cases} True & if\ Q_{raw} > Q_{start} \\ SF_{on_{prev}} & if\ Q_{raw} > Q_{min} \\ False & otherwise \end{cases} \quad (9)$$

$$Q_{out_{SF}} = \begin{cases} \min(Q_{defocus}, Q_{raw}) & if\ SF_{on} = True, defocus = True, Q_{defocus} < Q_{loss_{rec_{des}}} \\ 0 & if\ SF_{on} = True, defocus = True, Q_{defocus} < Q_{loss_{rec_{des}}} \\ Q_{raw} & if\ SF_{on} = True, defocus = False \\ 0 & if\ SF_{on} = False, defocus = False \end{cases} \quad (10)$$

$$damping = \begin{cases} Q_{out_{SF}}/Q_{raw} & if\ SF_{on} = True \\ 0 & if\ SF_{on} = False \end{cases} \quad (11)$$

$$W_{loss} = \begin{cases} n_{heliostat} \cdot he_{av} \cdot damping \cdot W_{track} & if\ ele > ele_{min} \\ 0 & otherwhise \end{cases} \quad (12)$$

$$Q_{wasted_{CSP}} = Q_{raw} - Q_{out_{SF}} \quad (13)$$

$$Q_{wasted_{startup}} = Q_{wasted_{CSP}} \cdot (1 - SF_{on}) \quad (14)$$

$$Q_{wasted_{defocus}} = Q_{wasted_{CSP}} - Q_{wasted_{startup}} \quad (15)$$

Table 6. Operation Outputs - heliostat field model

Symbol	Description	Unit
$Q_{in_{SF}}$	Input power in heliostat field	[W]
Q_{raw}	Raw heliostat field output power	[W]
$Q_{out_{SF}}$	Net heliostat field output power	[W]
$Q_{wasted_{startup}}$	Wasted heliostat field output power at startup mode	[W]
$Q_{wasted_{defocus}}$	Wasted heliostat field output power at defocus mode	[W]
$Q_{wasted_{CSP}}$	Total wasted heliostat field output power	[W]
SF_{on}	Boolean to indicate if the solar field is on	[-]
eta_{field}	Optical efficiency heliostat field	[-]
W_{loss}	Heliostat field parasitic loss	[W]

3.1.3. Receiver

The receiver model included in MoSES for P2P estimates the design and operation of the particle receiver using performance maps provided by CSPB as part of the parallel work in WP4. Particles are treated as the heat transfer fluid, with their properties either supplied by the user or estimated by default according to [10]. Similarly, receiver performance and thermal losses can be determined by interpolating lookup tables from CSPB or by applying the methodology proposed in [11], which accounts for natural and forced convection as well as radiation losses. Table 7 presents the parameters defining the receiver that needs to be customized by the user.

Table 7. Operation Outputs - heliostat field model

Description	Value	Unit	Ref.
Receiver outlet temperature	600-700	[◦C]	-
Back wall emissivity	0.8	[-]	[11]
Back wall thickness	0.05	[m]	[11]
Back wall conductivity	0.2	[W/(mK)]	[11]
Back wall heat transfer coefficient	10	[W/(m^{2}K)]	[11]
Particle diameter	350	[μm]	[12]
Particle specific heat	1200	[J/(kgK)]	[13]
Particle conductivity	2	[W/(mK)]	[13]

Particle density	3550	[kg/m^3]	[13]
Maximum solid volume fraction	0.6	[-]	[14]
Particle absorptivity	0.87	[-]	[15]
Particle emissivity	0.87	[-]	[16]

The Solar Multiple (SM) is a key design parameter to establish the ratio of the thermal power produced by the solar field to that required by the power block at the design point. The design receiver thermal output has been estimated as the product of the power block design thermal power ($Q_{PB,des}$) and the solar multiple, as shown in (16).

$$Q_{out,rec,des} = SM \cdot Q_{PB,des} \tag{16}$$

Design

Table 8 summarizes the main inputs required for the receiver design. The design outputs are estimated as shown in equations (17) – (32) and they are summarized in Table 9.

Table 8. Design Inputs – receiver model

Symbol	Description	Unit
$Medium$	HTF utilized in the receiver	[-]
$TLREC$	Thermal Losses Receiver Calculation - Model	[-]
$FlatPlate/Cavity$	Boolean to decide to use a flat plate/cavity receiver	[-]
$Q_{rec_{des}}$	Nominal output thermal power	[W]
$T_{out_{des}}$	Outlet HTF temperature at the design point	[K]
$T_{in_{des}}$	Inlet HTF temperature at the design point	[K]
$T_{amb_{des}}$	The ambient temperature at the design point	[K]
$u_{wind_{des}}$	Wind speed at the design point	[m/s]
H_{rec}	Receiver height	[m]
ar_{rec}	Receiver aspect ratio (height over width/diameter)	[-]
$geom_{inputs}$	Receiver geometrical inputs (Number of panels in the receiver,…)	[-]
$k_{material}$	The conductivity of the receiver material	[W/(mK)]
ab_{rec}	Receiver coating absorptance	[-]
em_{rec}	Receiver coating emissivity	[-]
$input_{eff}$	Boolean to decide to use a fixed receiver efficiency	[-]
$eta_{rec_{input}}$	Input of a constant receiver efficiency	[-]

$$state_{inlet_{des}} = Medium.setState_{pTX}(Medium.p_{default}, T_{in_{des}}) \tag{17}$$
$$state_{outlet_{des}} = Medium.setState_{pTX}(Medium.p_{default}, T_{out_{des}}) \tag{18}$$
$$h_{in_{des}} = f(state_{inlet_{des}}) \tag{19}$$
$$h_{out_{des}} = f(state_{outlet_{des}}) \tag{20}$$
$$m_{flow_{des}} = Q_{rec_{des}}/(h_{out_{des}} - h_{in_{des}}) \tag{21}$$
$$w_{rec} = H_{rec}/ ar_{rec} \quad if\ FlatPlate = True \tag{22}$$
$$D_{rec} = H_{rec}/ ar_{rec} \quad if\ FlatPlate = False \tag{23}$$
$$A_{receiver} = H_{rec} \cdot w_{rec} \quad if\ FlatPlate = True$$
$$A_{receiver} = \pi \cdot ar_{rec} \cdot D_{rec}^2 \quad if\ FlatPlate = False \tag{24}$$
$$eta_{rec_{des}} = \begin{cases} Q_{rec_{des}}/Q_{in_{rec_{des}}} & input_{eff} = False \\ eta_{rec_{input}} & otherwise \end{cases} \tag{25}$$
$$Q_{in_{rec_{des}}} = \begin{cases} Q_{absorbed}/ab_{rec} & input_{eff} = False \\ Q_{rec_{des}}/eta_{rec_{des}} & otherwise \end{cases} \tag{26}$$
$$Q_{absorbed} = Q_{rec_{des}} + Q_{adv_{loss_{des}}} + Q_{rad_{loss_{des}}} \tag{27}$$

$$Q_{adv\,loss_{des}} = TLREC\left(T_{amb_{des}}, Q_{rec_{des}}, T_{out_{des}}, T_{in_{des}}, u_{wind_{des}}, m_{flow_{des}}, Rec_{design}\right) \quad (28)$$

$$Q_{rad\,loss_{des}} = TLREC\left(T_{amb_{des}}, Q_{rec_{des}}, T_{out_{des}}, T_{in_{des}}, em_{rec}, m_{flow_{des}}, Rec_{design}\right) \quad (29)$$

$$Q_{rec\,loss_{des}} = (1 - ab_{rec}) \cdot Q_{in\,rec_{des}} \quad (30)$$

$$Q_{loss\,rec_{des}} = \begin{cases} Q_{rad\,loss_{des}} + Q_{adv\,loss_{des}} + Q_{rec\,loss_{des}} & input_{eff} = False \\ Q_{in\,rec_{des}} - Q_{rec_{des}} & otherwise \end{cases} \quad (31)$$

$$eta_{rec\,th_{des}} = Q_{rec_{des}} / Q_{absorbed} \quad (32)$$

Table 9. Design Outputs – receiver model

Symbol	Description	Unit
Rec_{design}	Complete geometrical design of the receiver*	[-]
$eta_{rec_{des}}$	Design total receiver efficiency	[-]
$eta_{rec\,th_{des}}$	Design thermal receiver efficiency	[-]
$Q_{loss\,rec_{des}}$	Design receiver losses	[W]
$Q_{in\,rec_{des}}$	Design receiver input power	[w]
$m_{flow_{des}}$	Design receiver mass flow rate	[kg/s]

* It summarizes all the geometrical parameters calculated above.

Operation

Operating Inputs – receiver model summarizes the main hourly inputs required for the estimation of the operating performance of the receiver. The outputs are estimated by using the equations (33) – (47) and they are summarized in Operating Outputs - receiver model.

Table 10. Operating Inputs – receiver model

Symbol	Description	Unit
$Medium$	HTF utilized in the receiver	[-]
$TLREC$	Thermal Losses Receiver Calculation - Model	[-]
$Q_{in\,rec}$	Incoming receiver power	[W]
h_{in}	Input specific enthalpy	[J/kg]
m_{flow}	Receiver mass flow rate	[kg/s]
SF_{on}	Boolean to indicate if the solar field is on	[-]
T_{amb}	Ambient temperature	[K]
u_{wind}	Wind speed	[m/s]
$T_{out_{des}}$	Set point output temperature	[K]
Rec_{design}	Receiver geometrical design	[-]
$rec_{absorptance}$	Receiver absorptance	[-]
$rec_{emissivity}$	Receiver emissivity	[-]
$input_{eff}$	Boolean to indicate if a fixed efficiency should be used	[-]
$eta_{rec_{input}}$	Input receiver efficiency (if input_eff is True)	[-]

$$state_{inlet} = Medium.setState_{phX}(Medium.p_{default}, h_{in}) \quad (33)$$

$$state_{outlet} = Medium.setState_{pTX}(Medium.p_{default}, T_{out_{des}}) \quad (34)$$

$$T_{in} = f(state_{inlet}) \quad (35)$$

$$h_{out,set} = f(state_{outlet}) \quad (36)$$

$$Q_{out_{rec_{guess}}} = m_{flow} \cdot (h_{out_{set}} - h_{in}) \quad (37)$$
$$Q_{adv_{loss}} = TLREC\left(T_{amb}, Q_{out_{rec_{guess}}}, T_{out_{des}}, T_{in}, u_{wind}, m_{flow}, Rec_{design}\right) \quad (38)$$
$$Q_{rad_{loss}} = TLREC\left(T_{amb}, Q_{out_{rec_{guess}}}, T_{out_{des}}, T_{in}, rec_{emissivity}, m_{flow}, Rec_{design}\right) \quad (39)$$
$$Q_{absorbed} = rec_{absorptance} \cdot Q_{in_{rec}} \quad (40)$$
$$Q_{ref_{loss}} = Q_{in_{rec}} - Q_{absorbed} \quad (41)$$
$$Q_{loss_{th_{rec}}} = Q_{rad_{loss}} + Q_{adv_{loss}} \quad (42)$$
$$Q_{loss_{rec}} = Q_{loss_{th_{rec}}} + Q_{ref_{loss}} \quad (43)$$
$$eta_{th_{rec}} = \left(Q_{absorbed} - Q_{loss_{th_{rec}}}\right)/Q_{absorbed} \quad (44)$$
$$eta_{rec} = \left(Q_{in_{rec}} - Q_{loss_{rec}}\right)/Q_{in_{rec}} \quad (45)$$
$$Q_{out_{rec}} = eta_{rec} \cdot Q_{in_{rec}} \quad (46)$$
$$h_{out} = h_{in} + Q_{out_{rec}}/m_{flow} \quad (47)$$

Table 11. Operating Outputs - receiver model

Symbol	Description	Unit
$Q_{out_{rec}}$	Output receiver power	[W]
h_{out}	Output specific enthalpy	[J/kg]
eta_{rec}	Receiver total efficiency	[-]
$eta_{th_{rec}}$	Receiver thermal efficiency	[-]
$Q_{loss_{rec}}$	Receiver thermal losses	[-]

3.1.4. Thermal Energy Storage

A two-silo thermal energy storage layout has been included in this tool: The design hot temperature should be set coherently with the receiver + EH assumption. The design cold temperature depends on the power block type selection and the return sCO_2 temperature. The energy stored can be calculated as a function of the hours of storage, and the design of thermal power to the power block.

Design

Table 12 summarizes the main inputs required for the thermal energy storage design. The design outputs are estimated as shown in equations (48) – (57) and they are summarized in Table 13.

Table 12. Design Inputs – thermal energy model

Symbol	Description	Unit
$Medium$	HTF utilized in the TES	[-]
$T_{cold_{set_{TES}}}$	Design cold temperature for TES	[K]
$T_{hot_{set_{TES}}}$	Design hot temperature for TES	[K]
$t_{storage}$	Storage hours	[h]
$Q_{flow_{des}}$	Design thermal power to the power block	[W]
$H_{storage}$	Storage tank height	[m]
$tank_{min_l}$	Minimum tank height	[m]

$$state_{cold,TES_{des}} = Medium.setState_{pTX}\left(Medium.p_{default}, T_{cold_{set_{TES}}}\right) \quad (48)$$
$$state_{hot,TES_{des}} = Medium.setState_{pTX}\left(Medium.p_{default}, T_{hot_{set_{TES}}}\right) \quad (49)$$
$$h_{cold_{set_{TES}}} \quad \rho_{cold_{set_{TES}}} = f\left(state_{cold,TES_{des}}\right) \quad (50)$$
$$h_{hot_{set_{TES}}} \quad \rho_{hot_{set_{TES}}} = f\left(state_{hot,TES_{des}}\right) \quad (51)$$

$$E_{max} = t_{storage} \cdot 3600 \cdot Q_{flow_{des}} \quad (52)$$
$$m_{max} = E_{max} / \left(h_{hot_{set_{TES}}} - h_{cold_{set_{TES}}} \right) \quad (53)$$
$$V_{max} = m_{max} / \rho_{ave_{TES}} \quad (54)$$
$$D_{storage} = \left(\frac{4 \cdot V_{max}}{\pi \cdot (H_{storage} - tank_{min_l})} \right)^{0.5} \quad (55)$$
$$V_{tank} = (H_{storage} \cdot \pi \cdot D_{storage}^2)/4 \quad (56)$$
$$A_{surf_{TES}} = \pi \cdot D_{storage} \cdot H_{storage} + \pi \cdot D_{storage}^2/4 \quad (57)$$

Table 13. Design Outputs – thermal energy storage model

Symbol	Description	Unit
E_{max}	Maximum tank stored energy	[J]
m_{max}	Maximum medium mass in tanks	[kg]
V_{tank}	Maximum medium volume in tanks	[m3]
$D_{storage}$	Storage tank diameter	[m]
$A_{surf_{TES}}$	Tank surface for losses	[m2]

Operation

Table 14 summarizes the main hourly inputs required for the estimation of the operating performance of the thermal energy storage. The outputs are estimated by using the equations (58) – (67) and they are summarized in Table 15.

Table 14. Operating Inputs – thermal energy storage model

Symbol	Description	Unit
$Medium$	HTF utilized in the TES	[-]
$m_{flow_{in}}$	Inlet mass flow rate in tank	[kg/s]
h_{in}	Inlet specific enthalpy	[J/kg]
m_{prev}	Previous value of estimated mass in tank	[kg]
h_{prev}	Previous value of average specific enthalpy	[J/kg]
$m_{flow_{out}}$	Outlet mass flow rate from tank	[kg/s]
T_{amb}	Ambient temperature	[K]
t_{in}	Initial time step	[s]
t_{out}	Final time step	[s]
dt	Duration time step	[s]
$Tank_{Design}$	Tank design parameters*	[-]
$m_{max_{des}}$	Maximum mass - design	[kg]
α	Tank heat transfer coefficient	[W/m2/K]
W_{aux}	Nominal heat tracing capacity	[W]
e_{ht}	Efficiency of the heat tracing system	[-]

* It summarizes all the geometrical parameters calculated above

$$state_{medium} = Medium.setState_{phX}(Medium.p_{default}, h_{prev}) \quad (58)$$
$$\frac{dm}{dt} = m_{flow_{in}} - m_{flow_{out}} \quad (59)$$
$$L = m/m_{max_{des}} \cdot 100 \quad (60)$$
$$T, \rho = f(state_{medium}) \quad (61)$$
$$V = m/\rho \quad (62)$$
$$A = \pi \cdot D_{storage} \cdot H_{storage} \cdot V/V_{tank} + \pi \cdot D_{storage}^2/4 \quad (63)$$
$$Q_{losses} = A \cdot \alpha \cdot (T - T_{amb}) \quad (64)$$
$$W_{net} = \min(Q_{losses}, W_{aux}) \quad (65)$$

$$W_{loss} = W_{net}/e_{ht} \quad (66)$$

$$m\frac{dh}{dt} + h\frac{dm}{dt} = m_{flow_{in}} \cdot h_{in} + m_{flow_{out}} \cdot h - Q_{losses} + W_{net} \quad (67)$$

Table 15. Operating Outputs – thermal energy storage model

Symbol	Description	Unit
L	Tank level	[%]
h	Average specific enthalpy	[J/kg]
m	Mass of HTF stored in the tank	[kg]
Q_{losses}	Thermal losses	[W]
W_{loss}	Parasitic losses due to heat	[W]

3.1.5. sCO2 Power Block

The power block model has been implemented in MoSES by interpolating design and part-load performance maps developed by POLIMI, in the parallel work conducted in WP4 for all the layouts presented in Figure 2. The user can select the power block by using four Booleans variables, 1 for each power block layout: *RCC, RCBC, RCIC,* and *PCC*. Dry cooling has been considered for all the configurations.

Design

Table 16 summarizes the main inputs required for the power block design. The design outputs are estimated directly from the lookup tables provided by POLIMI and they are summarized in Table 17. The isentropic efficiency of the turbine (eta_T) and the compressor (eta_C) are estimated iteratively as a function of the turbomachinery size.

Table 16. Design Inputs – sCO2 power block model

Symbol	Description	Unit
P_{gross}	Power Cycle Gross Output	[W]
TIT	Turbine Inlet Temperature at design	[K]
$T_{in_{Compr}}$	Compressor inlet temperature at design	[K]
p_{high}	Power block design high pressure	[Pa]
p_{low}	Power block design low pressure	[Pa]
eta_{gen}	Mechanical-to-Electrical Efficiency	[-]
eta_{HTR}	Effectiveness High-Temperature Recuperator	[-]
$T_{hot_{heater_{set}}}$	Heat source high-temperature design	[K]
$T_{cold_{heater_{set}}}$	Heat source low-temperature input value	[K]
$DT_{pinch_{hot-sCO2}}$	Initial Temperature difference for the primary HX(s)	[K]
$T_{in_{air_{cooler_{des}}}}$	The ambient temperature at design point for the power block	[K]
$DT_{recuperator}$	Min Pich-point temperature recuperators	[K]

Table 17. Design Outputs – sCO2 power block model

Symbol	Description	Unit
$m_{flow_{sCO2}}$	Design sCO2 Mass flow rate	[kg/s]
$eta_{blk_{des}}$	Design power block efficiency	[-]
$T_{sCO2_{cold_{des}}}$	Design return sCO2 temperature - MH	[K]
$T_{max_{HTR_{sCO2}}}$	Maximum temperature HTR	[K]

$W_{T1_{des}}$	Design HPT power	[W]
eta_{T1}	Design HPT isentropic efficiency	[-]
$W_{C1_{des}}$	Design MC1 power	[W]
eta_{C1}	Design MC1 isentropic efficiency	[-]
$UA_{MH_{des}}$	Overall heat transfer coefficient MH	[W/K]
$UA_{HTR_{des}}$	Overall heat transfer coefficient HTR	[W/K]
$UA_{cooler_{des}}$	Overall heat transfer coefficient cooler	[W/K]
$Q_{Cooler_{des}}$	Design cooler power	[W]
$DT_{pinch_{cooler}}$	Cooler pinch-point temperature difference	[K]
Q_{HTR}	Design HTR power	[W]
$cycle_{points}$	Thermodynamic states of all the cycle points	[-]

Operation

Table 18 summarizes the main hourly inputs required for the estimation of the operating performance of the power block. Similarly, also for the operation, the outputs are estimated by interpolating the lookup tables provided by POLIMI, and they are summarized in Table 19.

Table 18. Operating Inputs– sCO2 power block model

Symbol	Description	Unit
m_{flow}	sCO2 Mass flow rate - MH	[kg/s]
TIT	Turbine Inlet Temperature	[K]
$T_{in_{Compr_{des}}}$	Compressor inlet temperature	[K]
$eta_{HPT_{des}}$	Design HPT isentropic efficiency	[-]
$eta_{MC_{des}}$	Design MC1 isentropic efficiency	[-]
eta_{HTR}	Effectiveness High-Temperature Recuperator	[-]
eta_{gen}	Mechanical-to-Electrical Efficiency	[-]
$use_{eta_{net_{blk}}}$	Boolean to decide to use a fixed net-to-gross efficiency or calculate parasitic losses	[-]
$eta_{net_{blk}}$	Gross-to-net power conversion factor at the power block	[-]
T_{amb}	Ambient Temperature	[K]
$DT_{pinch_{cooler}}$	Cooler pinch-point temperature difference	[K]
$W_{base_{blk}}$	Fixed power block power consumption	[W]
$parasities_{blk}$	Parasitic losses	[W]
$DT_{recuperator}$	Min Pich-point temperature recuperators	[K]

Table 19. Operating Outputs – sCO2 power block model

Symbol	Description	Unit
W_{net}	Net power production	[W]
h_6	Return specific enthalpy - MH	[J/kg]
eff	Efficiency	[-]
Q_{Cooler}	Cooling thermal power	[W]
Q_{HTR}	HTR thermal power	[W]
W_{T1}	HPT power	[W]
W_{C1}	MC1 power	[W]
$cycle_{temperatures}$	Temperatures for the different cycle points	[-]

3.1.6. Electric Heater

The electric heater has been modeled with a fixed electric-to-thermal efficiency approach.

Design

Table 20 summarizes the main inputs required for the electric heater design. The design outputs are estimated as shown in equations (68) – (73) and they are summarized in Table 21.

Table 20. Design Inputs – electric heater model

Symbol	Description	Unit
$Medium$	HTF utilized in the electric heater	[-]
$eta_{heater_{des}}$	Electric-to-thermal efficiency	[-]
$T_{out_{des}}$	Outlet HTF temperature at the design point	[K]
$T_{in_{des}}$	Inlet HTF temperature at the design point	[K]
$P_{name_{EH}}$	Net electric heater power	[W]

$$Q_{name_{EH}} = P_{name_{EH}} \cdot eta_{heater_{design}} \tag{68}$$

$$state_{inlet_{EH_{des}}} = Medium.setState_{pTX}(p_{default}, T_{in_{des}}) \tag{69}$$

$$state_{outlet_{EH_{des}}} = Medium.setState_{pTX}(p_{default}, T_{out_{des}}) \tag{70}$$

$$h_{cold_{set_{EH}}} = f\left(state_{inlet_{EH_{des}}}\right) \tag{71}$$

$$h_{hot_{set_{EH}}} = f\left(state_{outlet_{EH_{des}}}\right) \tag{72}$$

$$m_{flow_{EH_{des}}} = Q_{name_{EH}} / \left(h_{hot_{set_{EH}}} - h_{cold_{set_{EH}}}\right) \tag{73}$$

Table 21. Design Outputs – electric heater model

Symbol	Description	Unit
$P_{name_{EH}}$	Nominal electric power	[W]
$Q_{name_{EH}}$	Nominal thermal power	[W]
$m_{flow_{EH_{des}}}$	Design mass flow rate	[kg/s]

Operation

Table 22 summarizes the main hourly inputs required for the estimation of the operating performance of the electric heater. The outputs are estimated by using the equations (74) – (76) and they are summarized in Table 23.

Table 22. Operating Inputs – electric heater model

Symbol	Description	Unit
W_{heater}	Net Power to the electric heater	[W]
h_{in}	Inlet specific enthalpy	[J/kg]
m_{flow}	Mass flow rate	[kg/s]
eff_heater	Electric-to-thermal efficiency	[-]
EH_{on}	Boolean to indicate if electric heater is on	[-]

$$Q_{loss_{heater}} = \begin{cases} P_{PV_{heater}} \cdot \left(1 - eta_{heater_{design}}\right) & if\ EH_{on} = True \\ 0 & otherwise \end{cases} \tag{74}$$

$$Q_{out_{heater}} = eta_{heater} \cdot P_{PV_{heater}} \tag{75}$$

$$h_{out} = h_{in} + Q_{out_{heater}} / m_{flow} \tag{76}$$

Table 23. Operating Outputs – electric heater model

Symbol	Description	Unit
$Q_{out_{heater}}$	Thermal power output	[W]
h_{out}	Output specific enthalpy	[J/kg]
$Q_{loss_{heater}}$	Thermal power losses	[W]

3.1.7. PV Plant

The PV plant has been modeled using the module Pvwattsv8 included in the tool NREL-PySAM. The design and operating conditions are estimated simultaneously. The system is designed with a scalable size in terms of the number of inverters to reach the nominal PV capacity (in MWAC), with a fixed DC-AC ratio. Table 24 summarizes the main design and operating inputs required for the estimation of the operating performance of the PV field. The outputs are estimated by using the equations (77) – (82) and they are summarized in 0.

Table 24. Inputs – PV model

Symbol	Description	Unit
w_{file}	Weather File	[-]
$azimuth$	Array azimuth angle [deg] - Options: N=0, E=90,S=180,W=270	[deg]
$array_{type}$	Array type [0, 1, 2, 3, 4] - [Fixed Rack, Fixed Roof, 1Axis, Backtracked, 2Axis]	[-]
$bifaciality$	Module bifaciality factor [0 or ~0.65]	[-]
r_{DCAC}	DC-to-AC ratio	[-]
$en\_snowloss$	Boolean to enable snow loss model	[-]
en_wind_stow	Boolean to enable tracker stow at high wind speeds	[-]
GCR	Ground coverage ratio	[-]
$tilt$	Array tilt angle (if no tracking)	[deg]
$eta_{inv_{input}}$	Inverter efficiency at rated power	[-]
tot_DC_losses	Total DC losses, Total system losses	[-]
$module_{type}$	Module type [0, 1, 2] - [Standard,Premium,Thin film]	[-]
rot_lim	Tracker rotation angle limit	[deg]
$stow\_wspd$	Tracker stow wind speed threshold	[m/s]
P_{DC}	DC nameplate system capacity	[W]
$tilt$	Array tilt angle (if no tracking)	[deg]
$wind\_stow\_angle$	Tracker angle for wind stow	[deg]
$P_{single_{PV}}$	Single PV module DC power output	[W]
eff_single_PV	Single PV Efficiency	[-]

$$A_{PV_{field}} = P_{DC}/eff_{single_{PV}} \quad (77)$$

$$N_{PV_{modules}} = A_{PV_{field}}/1.7/2 \quad (78)$$

$$A_{land_{PV_{tot}}} = A_{land_{PV_{tot}}} = 1.7 * \left(\frac{3}{GCR}\right) * N_{PV_{modules}} \quad (79)$$

$$EnergyYield_{PV} = output\ from\ PySAM \quad (80)$$

$$P_{DC_{inv}} = output\ from\ PySAM \quad (81)$$

$$W_{tot_{PV}} = output\ from\ PySAM \quad (82)$$

Table 25. Outputs – PV model

Symbol	Description	Unit
$A_{land_{PV_{tot}}}$	Total land occupied by the PV plant	[m2]
$A_{PV_{field}}$	Land occupied by PV modules	[m2]
$EnergyYield_{PV}$	Energy Yield PV plant	[kWh/kW]
CF_{PV}	Capacity Factor PV plant	[%]
$P_{DC_{inv}}$	Power DC output	[W]
$W_{tot_{PV}}$	Total Power AC output	[W]

3.1.8. Battery Energy Storage System

The Battery energy storage system plant has been modeled incorporating the aging effects of the BESS, accounting for both calendar and cycle degradation [16]. Replacement of the BESS is considered when its health—defined as 100% when corresponding to the installed energy capacity for charge and discharge—falls below 50% due to actual usage patterns. The design and operating conditions are estimated simultaneously. Table 26 summarizes the main design and operating inputs required for the estimation of the operating performance of the BESS. The outputs are estimated by using the equations (83) – (105) and they are summarized in Table 27.

Design and Operation

Table 26. Design and Operation Inputs – BESS model

Symbol	Description	Unit
$t\_storage$	Battery Capacity in hours of storage	h
$P\_AC\_BESS_{des}$	Design AC Power to Grid from BESS	W-AC
eta_inv_{des}	Design and Operation - Inverter Efficiency	-
$eta\_BESS\_RT_{des}$	Initial Roundtrip DC Efficiency	-
$DOD\_max_{initial}$	Initial Maximum DOD of BESS	-
$Degradation\_E\_BESS_{calendar}$	Calendar Degradation	-/year
$Degradation\_E\_BESS_{cycle}$	Cycling Degradation	/cycle
$Degradation\_eta\_BESS\_RT_{calendar}$	Roundtrip DC Efficiency Calendar Degradation	-/year
$Degradation\_eta\_BESS\_RT_{cycle}$	Roundtrip DC Efficiency Cycling Degradation	/cycle
P_grid_{limit}	Grid interconnection limit	W-AC
$P\_charge\_AC_{RES}$	AC Power from RES to BESS	W-AC
$P\_charge\_AC_{grid}$	AC Power from grid to BESS	W-AC
$P\_discharge\_AC_{set}$	AC Power from BESS to grid - set point	W-AC
SOC_{prev}	State of Charge at the previous time step	-
$E\_BESS\_DC\_usable\_prev$	Usable Battery bank - at each time step	Wh-DC
$E\_DC\_discharged_{fromBESS_{prev}}$	DC Electricity discharged from BESS prev	Wh-DC
$delta\_t$	Time step simulated	[s]
$SystemAge\_prev$	Age of the BESS System	years
$share\_degCycle\_E\_BESS_{prev}$	Share of Cycle Degradation of BESS prev	-
$share\_degCycle\_RTDC_{eff_{prev}}$	Share of Cycle Degradation of RT Efficienc prev	-

$$P_{AC_{BESS_{des}}} = P_{AC_{BESS_{des}}} \tag{83}$$

$$P_{AC_{BESS_{des}}} = \frac{P_{AC_{BESS_{des}}}}{eta\_inv_{des}} \tag{84}$$

$$E_{BESS_{DC_{nom_{des}}}} = P_{DC_{BESS_{des}}} * t_{storage}/DOD_{max} \tag{85}$$

$$E_{BESS_{DC_{usable_{des}}}} = P_{DC_{BESS_{des}}} * t_{storage} \tag{86}$$

$$BESS_h = E_{BESS_{DC_{usable_{des}}}} * eta_{inv_{des}} / P_{AC_{BESS_{des}}} \quad (87)$$

$$SystemAge = delta_t/(3600 * 8760) + SystemAge_{prev} \quad (88)$$

$$share_{BESS_{cycle}} = E_{DC_{discharged_{fromBESS_{prev}}}} / E_{BESS_{DC_{usable_{prev}}}} \quad (89)$$

$$share_{degCycle_{E_{BESS}}} = share_{degCycle_{E_{BESS_{prev}}}} + (Deg_{E_{BESS_{cycle}}} * share_{BESS_{cycle}}) \quad (90)$$

$$share_{degCalendar_{E_{BESS}}} = Degradation_{E_{BESS_{calendar}}} * SystemAge \quad (91)$$

$$E_{BESS_{DC_{usable}}} = E_{BESS_{DC_{usable_{des}}}} * (1 - (sh_{degCycle_{E_{BESS}}} + sh_{degCalendar_{E_{BESS}}})) \quad (92)$$

$$sh_{degCycle_{RTDC_{eff}}} = sh_{degCycle_{RTDC_{eff_{prev}}}} + \left(Deg_{eta_{BESS_{RT_{cycle}}}} * share_{BESS_{cycle}}\right) \quad (93)$$

$$sh_{degCalendar_{RTDC_{eff}}} = Deg_{eta_{BESS_{RT_{calendar}}}} * SystemAge \quad (94)$$

$$eta_{BESS_{RT}} = eta_{BESS_{RT_{des}}} * \left(1 - \left(share_{degCycle_{RTDC_{eff}}} + share_{degCalendar_{RTDC_{eff}}}\right)\right) \quad (95)$$

$$BESS_{health} = \frac{E_{BESS_{DC_{usable}}}}{E_{BESS_{DC_{usable_{des}}}}} \quad (96)$$

$$W_{AC_{toBESS}} = W_{AC_{RES_{toBESS}}} + W_{AC_{grid_{toBESS}}} \quad (97)$$

$$W_{DC_{toBESS}} = W_{AC_{toBESS}} * eta_{BESS_{RT}} * eta_{inv_{des}} \quad (98)$$

$$W_{DC_{fromBESS}} = W_{AC_{fromBESS}} / eta_{inv_{des}} \quad (99)$$

$$SOC = SOC_{prev} + \left(W_{DC_{toBESS}} - W_{DC_{fromBESS}}\right) * \frac{delta_t}{E_{BESS_{DC_{usable}}}} \quad (100)$$

$$W_{BESS_{to_{grid}}} = W_{DC_{fromBESS}} * eta_{inv_{des}} \quad (101)$$

$$W_{system_{to_{BESS}}} = W_{AC_{RES_{toBESS}}} \quad (102)$$

$$W_{grid_{to_{BESS}}} = W_{AC_{grid_{toBESS}}} \quad (103)$$

$$E_{DC_{discharged_{fromBESS}}} = W_{DC_{fromBESS}} * \frac{delta_t}{3600} \quad (104)$$

$$E_{DC_{charged_{toBESS}}} = W_{DC_{toBESS}} * \frac{delta_t}{3600} \quad (105)$$

Table 27. Design and Operation Outputs – BESS model

Symbol	Description	Unit
P_AC_BESS_des	Battery Power - Inverter design power	W-AC
BESS_h	Battery Capacity in hours of storage	h
E_BESS_DC_nom_des	Nameplate Battery bank installed capacity	Wh-DC
E_BESS_DC_usable_des	Usable Battery bank installed capacity	Wh-DC
W_BESS_to_grid	AC Electric Power to grid from battery	W-AC
W_system_to_BESS	AC Electric Power to battery from system	W-AC
W_grid_to_BESS	AC Electric Power to battery from grid	W-AC
SOC	Battery state of charge	%
E_DC_discharged_fromBESS	DC Electricity discharged from BESS	Wh-DC
E_DC_charged_toBESS	DC Electricity charged to BESS	Wh-DC
E_BESS_DC_usable	Usable Battery bank - at each time step	Wh-DC
eta_BESS_RT	Battery average roundtrip efficiency	-
SystemAge	Age of the BESS System	years
BESS_health	Percentage of usable capacity compared to start	-
share_degCycle_E_BESS	Previous Share of Cycle Degradation of BESS Energy	-
share_degCycle_RTDC_eff	Previous Share of Cycle Degradation of RT Efficiency	-

3.2. Financial cost model

Two main economic indicators have been considered: capital investment cost (CAPEX) and operational cost (OPEX). The capital investment includes the direct and indirect costs for all the main components identified in the solar plant. The operational cost accounts for the operation and maintenance of the plant, distinguishing production-dependent and capacity-dependent yearly costs. Table 28 summarizes the cost assumptions for the main components identified in the hybrid plant. The considered cost functions are also reported in this section. The cost assumptions have been converted into EUR, considering the average 2021 USD-to-EUR exchange rate of 0.84 [17]. A nominal discount rate (d) of 7% and an interest rate (i) of 2.5% can be adopted [18]. A plant operational lifetime (N) of 30 years is suggested to be considered for the PV-CSP plant [18]. All of the financial indicators mentioned above are customizable, and the provided values are only reference points. Similarly, the costs listed below serve as reference values that the user can adjust or replace with actual component costs.

Table 28. Cost assumptions for the hybrid PV-CSP plant.

	Description	Unit	Value	Ref.
Heliostat field Tower and Receiver	Heliostat field	EUR/m^2	100	[19]
	Tower reference cost	MEUR	2.5	[20]
	Tower cost exponent	-	0.0113	[20]
	Receiver specific	kEUR/ m^2	31.4	[10]
Particle Lift	Lift specific	EUR/(kg/s-m)	49	[10]
Storage	Particle bin specific	EUR/m^2	1033	[10]
	Particles	EUR/kg	0.84	[10]
	Particle loss per year	-	0.0001	[10]
	Non-storage inventory	-	0.05	[10]
sCO_2 Power Block	Particle-to-sCO_2 HX	EUR/(W/K)$^{0.8778}$	14.7	[21]
	sCO_2 turbine	kEUR/(MW)$^{0.5561}$	153	[22]
	sCO_2 compressor	kEUR/(MW)$^{0.3992}$	1033	[22]
	sCO_2-sCO_2 recuperator	EUR/(W/K)$^{0.7544}$	41.5	[22]
	sCO_2-Air cooler	EUR/(W/K)$^{0.75}$	27.6	[22]
	Gearbox	kEUR/(MW)$^{0.2434}$	149	[22]
	Generator	kEUR/(MW)$^{0.5463}$	92	[22]
	sCO_2 piping	%PB cost	15 (20)	[22]
Electric Heater	Fixed Cost	EUR/kW$_e$	125	*
	Variable Cost	EUR/kW$_e$	15	*
PV	Module	EUR/W$_{DC}$	0.24	[23]
	Balance of System	EUR/W$_{DC}$	0.18	[24]
	Inverter	EUR/W$_{AC}$	0.04	[24]
Battery Energy Storage System	Balance of system	EUR/W$_{AC}$	0.08	[23]
	Power control system	EUR/W$_{AC}$	0.06	[23]
	Energy Storage	EUR/Wh$_{AC}$	0.18	[23]
	Replacement	EUR/Wh$_{AC}$/N$_{rep}$	0.12	[23]
Other-CSP	Balance of Plant	EUR/kW$_e$	244	[20]
	Contingency	%direct costs	7	[20]
	EPC	%direct costs	13	[20]
	Fixed O&M – cap	EUR/kW-yr	34	[20]
	Variable O&M – gen	EUR/MWh-yr	3	[20]
Other-PV	Contingency	%direct costs	5	[24]
	EPC	%direct costs	10	[24]
	Fixed O&M – cap	EUR/kW-yr	11	[24]
	Variable O&M – gen BESS	EUR/MWh$_{AC}$	1.8	[23]

	Fixed O&M – cap BESS	EUR/kW$_{AC}$	5.8	[23]
Land	Land	EUR/m^2	2.1	[20]
	Site Improvement	EUR/m^2	8.4	[20]

[*] based on a real quotation

In this section, the adopted financial cost model is presented. The overall investment cost of a hybrid CSP-PV plant under investigation is estimated as the sum of the CAPEX of the CSP and PV plant, as shown in equation (106). Similarly, the operating expenditure (OPEX) is calculated as shown in equation (107). Each of these parameters can be estimated using the cost functions for the single components as functions of the sizes or can be provided directly from the user.

$$CAPEX = CAPEX_{CSP} + CAPEX_{PV} + CAPEX_{BESS} \quad (106)$$

$$OPEX = OPEX_{CSP} + OPEX_{PV} + OPEX_{BESS} \quad (107)$$

3.2.1. CSP Plant

The capital expenditure of the CSP plant (including an eventual electric heater) can be estimated as the sum of the direct and indirect costs of the plant:

$$CAPEX_{CSP} = C_{d,CSP} + C_{ind,CSP} \quad (108)$$

3.2.1.1. Direct Costs

The direct costs of the plant include all the subsystems costs that have been identified in the system layout, as shown in equation (109). These include the solar field (*SF*), the site improvement (*site*), the tower (*tower*), the receiver (*rec*), the particle lift (*lift*), the thermal energy storage (*TES*), the balance of plant (*BOP*), the electric heater (*EH*), the power block (*PB*), and the contingencies ($f_{cont,CSP}$).

$$C_{d,CSP} = \left(C_{SF} + C_{site} + C_{tower} + C_{rec} + C_{lift} + C_{TES} + C_{BOP} + C_{EH} + C_{PB}\right) \cdot \left(1 + f_{cont,CSP}\right) \quad (109)$$

These contributions to the total direct costs of the plant are evaluated in equations (110) - (124). The contingency costs are estimated just as a fraction of the other direct costs. The specific or reference costs are dependent on the media adopted in the CSP field. For each layout under investigation, these values are pre-set based on the literature and can be customized by the user.

$$C_{SF} = c_{SF} \cdot A_{SF} \quad (110)$$

$$C_{site} = c_{site} \cdot A_{SF} \quad (111)$$

$$C_{tower} = C_{tower,ref} \cdot e^{tower,exp \cdot H\_tower} \quad (112)$$

$$C_{rec} = c_{rec} \cdot A_{rec} \quad (113)$$

$$C_{lift} = c_{lift} \cdot m_{flow_{particle_{des}}} \cdot H_{tower} \quad (114)$$

$$c_{bin_{hot}} = c_{bin_{spec}} \cdot (1 + 0.3 \cdot \left(\left(T_{hot_{set_{TES}}}[°C]\right) - 600\right) / 400)) \quad (115)$$

$$c_{bin_{cold}} = c_{bin_{spec}} \cdot (1 + 0.3 \cdot \left(\left(T_{cold_{set_{TES}}}[°C]\right) - 600\right) / 400)) \quad (116)$$

$$C_{particle} = c_{particle} \cdot (1 + NS) \cdot m_{particle} \quad (117)$$

$$C_{particle_{loss}} = f_{loss_{particle}} \cdot t_{life} \cdot c_{particle} \cdot m_{flow_{particle_{des}}} \cdot 0.6 \cdot 8760 \cdot 3600 \quad (118)$$

$$C_{TES} = c_{bin_{hot}} \cdot A_{surf_{TES}} + c_{bin_{cold}} \cdot A_{surf_{TES}} + C_{particle} + C_{particle_{loss}} \quad (119)$$

$$C_{BOP} = c_{BOP} \cdot P_{gross} \quad (120)$$

$$f_{T,EH} = 2.68 \cdot \log\big(T_{max,EH}[°C]\big) - 16 \qquad if\ T_{max,EH} > 550\ °C \quad (121)$$

$$f_{T,EH} = 1 \qquad if\ T_{max,EH} \leq 550\ °C \quad (122)$$

$$C_{EH} = (c_{EH,fixed} + c_{EH,var} \cdot f_{T,EH}) \cdot P_{EH,des} \quad (123)$$

$$C_{PB} = C_{equipment,PB} + C_{piping} \quad (124)$$

The power block cost is estimated considering the cost of all the pieces of equipment involved as presented in (125). Equations (126) - (135) show the implemented cost functions for the sCO2 power block components.

$$C_{equipment,PB} = C_{MC1} + C_{MC2} + C_{RC} + C_{HPT} + C_{LPT} + C_{MH} + C_{RH} + C_{HTR} + C_{LTR} + C_{cooler} + C_{intercooler} + C_{generator} + C_{gearbox} \quad (125)$$

$$C_{MC1}, C_{MC2}, C_{RC} = C_{comp,ref} \cdot W_{comp,des}^{0.3992} \quad (126)$$

$$C_{HPT}, C_{LPT} = f_{T,turb} \cdot C_{turb,ref} \cdot W_{turb,des}^{0.5561} \quad (127)$$

$$f_{T,turb} = 1 + (1.106 \cdot 10^{-4} \cdot (TIT\ [°C] - 550)^2) \quad (128)$$

$$C_{MH}, C_{RH} = C_{heater,ref} \cdot UA_{heater,des}^{0.8778} \quad (129)$$

$$C_{HTR}, C_{LTR} = f_{T,recup} \cdot C_{recup,ref} \cdot UA_{recup,des}^{0.7544} \quad (130)$$

$$f_{T,recup} = 1 + 0.02141 \cdot (T_{max}\ [°C] - 550) \quad (131)$$

$$C_{cooler}, C_{intercooler} = C_{cooler,ref} \cdot UA_{cooler,des}^{0.75} \quad (132)$$

$$C_{generator} = C_{gen,ref} \cdot W_{gen,des}^{0.5463} \quad (133)$$

$$C_{gearbox} = C_{gearbox,ref} \cdot W_{turb/comp,des}^{0.2434} \quad (134)$$

$$C_{piping} = f_{piping} \cdot C_{equipment,PB} \quad (135)$$

3.2.1.2. Indirect Costs

The indirect costs of the plant include the engineering, procurement, and construction (EPC) costs, and the land cost (*land,CSP*) as shown in equation (136). The EPC costs are estimated as a fraction of the direct costs.

$$C_{ind,CSP} = C_{d,CSP} \cdot f_{EPC,CSP} + C_{land,CSP} \quad (136)$$

where $C_{land,CSP}$ is estimated as a function of the total land occupied by the CSP field:

$$C_{land,CSP} = c_{land} \cdot A_{tot,CSP} \quad (137)$$

3.2.1.3. Operating Costs

The operating costs account for the operation and maintenance of the plant distinguishing production-dependent ($c_{OM,prod,CSP}$) and capacity-dependent ($c_{OM,fix,CSP}$) yearly costs. Then, the OPEX can be calculated as shown in Equation (138) as a function of the installed capacity (P_{net}) and of the annual energy yield (AEY_{CSP}).

$$OPEX_{CSP} = c_{OM,fix,CSP} \cdot P_{net} + c_{OM,prod,CSP} \cdot AEY_{CSP} \tag{138}$$

3.2.2. PV Plant

The capital expenditure of the PV plant (including the inverter) can be estimated as the sum of the direct and indirect costs:

$$CAPEX_{PV} = C_{d,PV} + C_{ind,PV} \tag{139}$$

3.2.2.1. Direct Costs

The direct costs of the PV plant include all the subsystems costs that have been identified in the system layout, as shown in equation (140). These include the PV modules (*modules,PV*), the balance of the system (*BoS,PV*), the site improvement cost (*site,PV*), the inverters (*inverter,PV*), and the contingencies ($f_{cont,PV}$).

$$C_{d,PV} = \left(C_{modules,PV} + C_{BoS,PV} + C_{site,PV} + C_{inverter,PV}\right) \cdot \left(1 + f_{cont,PV}\right) \tag{140}$$

These contributions to the total direct costs of the plant are evaluated in equations (141) – (206). The contingency costs are estimated just as a fraction of the other direct costs. The specific or reference costs are dependent on the type of PV modules adopted in the plant, and on the tracking system. For each layout under investigation, these values are pre-set based on the literature and can be customized by the user.

$$C_{modules,PV} = c_{modules} \cdot P_{DC,PV} \tag{141}$$

$$C_{BoS,PV} = c_{BoS} \cdot P_{DC,PV} \tag{142}$$

$$C_{site,PV} = c_{site} \cdot A_{PV,field} \tag{143}$$

$$C_{inverter,PV} = c_{inverter} \cdot P_{AC,PV} \tag{144}$$

3.2.2.2. Indirect Costs

The indirect costs of the plant include the engineering, procurement, and construction (*EPC,PV*) costs, and the land cost (*land,PV*) as shown in equation (145). The EPC costs are estimated as a fraction of the direct costs.

$$C_{ind,PV} = C_{d,PV} \cdot f_{EPC,PV} + C_{land,PV} \tag{145}$$

where $C_{land,PV}$ is estimated as a function of the total land occupied by the PV field:

$$C_{land,PV} = c_{land} \cdot A_{PV,field} \tag{146}$$

3.2.2.3. Operating Costs

The operating costs account for the operation and maintenance of the plant considering only capacity-dependent ($c_{OM,fix,PV}$) yearly costs. The OPEX can be calculated as shown in equation (147) as a function of the installed capacity ($P_{AC,PV}$).

$$OPEX_{PV} = c_{OM,fix,PV} \cdot P_{AC,PV} \tag{147}$$

3.2.3. BESS

The capital expenditure of the BESS plant (including the inverter) can be estimated as the sum of the direct and indirect costs:

$$CAPEX_{BESS} = C_{d,BESS} + C_{ind,BESS} \quad (148)$$

3.2.3.1. Direct Costs

The direct costs of the BESS plant include all the subsystems costs that have been identified in the system layout, as shown in equation (149). These include the energy storage (ES,BESS), power conversion system (PCS,BESS), the balance of the system (*BoS,BESS*), the replacement cost (replacement,BESS), and the contingencies ($f_{cont,PV}$).

$$C_{d,BESS} = \left(C_{BoS_{BESS}} + C_{PCS_{BESS}} + C_{ES_{BESS}} + C_{replacement_{BESS}}\right) \cdot (1 + f_{cont,BESS}) \quad (149)$$

These contributions to the total direct costs of the plant are evaluated in equations (150) – (153). The contingency costs are estimated just as a fraction of the other direct costs. For each layout under investigation, these values are pre-set based on the literature and can be customized by the user.

$$C_{ES,BESS} = c_{ES,BESS} \cdot E_{BESS} \quad (150)$$

$$C_{BoS,BESS} = c_{BoS,BESS} \cdot P_{AC_{BESS_{des}}} \quad (151)$$

$$C_{PCS,BESS} = c_{PCS,BESS} \cdot P_{AC_{BESS_{des}}} \quad (152)$$

$$C_{replacement,BESS} = c_{replacement,BESS} \cdot E_{BESS} \cdot N_{replacement} \quad (153)$$

3.2.3.2. Indirect Costs

The indirect costs of the plant include the engineering, procurement, and construction (*EPC, BESS*) costs, as shown in equation (154). The EPC costs are estimated as a fraction of the direct costs.

$$C_{ind,BESS} = C_{d,BESS} \cdot f_{EPC,BESS} \quad (154)$$

3.2.3.3. Operating Costs

The operating costs account for the operation and maintenance of the plant distinguishing production-dependent ($c_{OM,prod,BESS}$) and capacity-dependent ($c_{OM,fix,BESS}$) yearly costs. Then, the OPEX can be calculated as shown in Equation (155) as a function of the BESS installed capacity ($P_{AC_{BESS_{des}}}$) and of the annual energy yield (AEY_{BESS}).

$$OPEX_{BESS} = c_{OM,fix,BESS} \cdot P_{AC_{BESS_{des}}} + c_{OM,prod,BESS} \cdot AEY_{BESS} \quad (155)$$

4. Key Performance Indicators

The list of the selected KPIs is provided in Table 29. For each KPI, a brief description is included too. For all of the defined KPIs, a more detailed definition and the corresponding equation is presented in the following section.

Table 29. List of selected Key Performance Indicators

KPI number	Key Performance Indicator (KPI) definition
	Technical
1	**Annual average Solar-to-Electricity efficiency (η_{ste}) [%]** The Solar-to-electric conversion efficiency measures the ability of the power plant to transform the primary solar resource into electricity.
2	**Annual average Receiver efficiency (η_{rec}) [%]** The receiver efficiency measures the ability of the receiver to convert the solar resource concentrated on the receiver into output thermal power.
3	**Power Block design efficiency (η_{PB}) [%]** The power block efficiency measures the ability of the power block to convert thermal power into electric power at the design condition.
4	**Power Block Off-design efficiency ($\eta_{PB,off}$) [%]** The power block off-design efficiency measures the ability of the power block to convert thermal power into electric power during off-design conditions. This KPI is provided as three efficiency values calculated for operating powers equal to 25%, 50%, and 75% of the design power.
5	**Storage efficiency (η_{TES})** The Thermal Energy Storage (TES) efficiency measures the ability of the storage to store the thermal energy over a specified period.
6	**Capacity Factor (CF) [%]** The Capacity Factor is a measure of how much energy is produced by a plant compared to its maximum output based on the installed capacity.
7	**Hybrid Capacity Factor (HCF) [%]** The Capacity Factor is a measure of how much energy is produced by a plant compared to its maximum output based on the load to fulfill.
8	**Availability Factor (AF) [%]** The availability factor is a measure of the availability of a power plant indicating the fraction of time that it can produce electricity over a certain period.
9	**Capacity Value (CV) [MW]**

	The Capacity Value measures the contribution of a power plant to reliably meeting demand. The capacity value is the contribution that a plant makes toward the planning reserve margin and it is expressed in terms of physical capacity (MW).
10	**HTF Maximum Temperature ($T_{max,HTF}$) [ºC]** The Heat Transfer Fluid (HTF) maximum temperature is the maximum temperature of the working fluid flowing into the receiver. It's a measure of the highest quality thermal power available in the plant and it can be used to compare different layouts of the CSP plant.
11	**HTF Temperature Difference (ΔT_{HTF}) [ºC]** The Heat Transfer Fluid (HTF) temperature difference coupled with the $T_{max,HTF}$ characterizes the receiver temperature design conditions and it is a measure of how compact the receiver can be.
12	**Storage Utilization Factor (UF_{TES}) [%]** The storage utilization factor is an indicator that identifies whether the storage size used for a particular configuration is too big or too small in terms of capacity.
13	**Annual Energy Yield (AEY) [GWh]** The annual energy yield provides the total annual electricity generation of the power plant.
14	**PV-direct-share of Electricity Produced per Year ($f_{PV,AEY}$) [%]** The PV-share of AEY is a KPI that quantifies how much the PV-field impacts on the total electricity production of a hybrid PV+CSP plant.
15	**Power Block Ramping Capability (RC_{PB}) [MW/hour]** The ramping capability provides an estimate of how well the power block can adjust its power output to changing load requirements or market conditions. Upward and downward ramping are assessed separately.
16	**Power Block Start-up Duration (SUD_{PB}) [hours]** The start-up duration is a measure of the period needed by the power block to reach the desired power output from off mode.
17	**Power Block Shut-down Duration (SDD_{PB}) [hours]** The shut-down duration is a measure of the period needed by the power block to reach the off mode from the operating power output condition.
18	**Flexibility Factor (FF) [-]** The flexibility factor indicates the ability to shift energy production from low to high price periods.
Economic	
19	**Capital Expenditure ($CAPEX$) [MEUR]**

	This KPI indicates the total investment required for the CSP plant or hybrid configuration CSP-PV-BESS for the different layouts under investigation, including direct and indirect costs.
20	**PV-share of CAPEX ($f_{PV,CAPEX}$) [%]** The PV-share of CAPEX is a KPI that quantifies how much the PV-field impacts on the total investment cost of a hybrid PV+CSP plant.
21	**Operational Expenditure ($OPEX$) [MEUR/year]** The OPEX relates to the operational and maintenance costs incurred during the operation of the power plant. These include fixed costs and production-dependent costs.
22	**Specific CAPEX (S_{CAPEX}) [EUR/MW]** The specific CAPEX is the investment cost per unit of installed capacity. This KPI can be used to compare large-scale and small-scale configurations based on their investment cost.
23	**Specific Cost of Thermal Energy Storage (SC_{TES}) [EUR/MWh$_{th}$]** The specific cost of the Thermal Energy Storage (TES) system quantifies the cost of storing a unit of thermal energy.
24	**Specific cost of the HTF system (SC_{HTF}) [EUR/kWth]** The specific cost of the Heat Transfer Fluid (HTF) system quantifies the cost of a unit of thermal energy converted from solar irradiation in the receiver, exchanged in intermediate heat exchangers (if any), and to be stored.
25	**Share of cost of conventional components ($f_{con,CAPEX}$) [%]** The share of the cost of the conventional components quantifies the impact of conventional components on the total investment cost of a solar-based renewable energy plant. This KPI is also a measure of what drives the CAPEX the most: conventional or innovative components.
26	**Specific Cost of Power Block (SC_{PB}) [EUR/kW]** The specific cost of the power block quantifies the cost of a unit of installed electric power capacity.
Environmental	
27	**Specific Water Consumption (SWC) [m^3/GWh]** The Specific Water Consumption (SWC) is calculated as the ratio between the total water demand and the electricity produced per year. The total water demand of the CSP or hybrid CSP+PV plant is estimated as the sum of the water required by the cooling system, by the mirrors cleaning system, plus a miscellaneous term considering power block make-up water, service water, sanitary/sewage water etc.
28	**Annual saving of $CO_{2,eq}$ emissions ($\Delta CO_{2_{eq}}$) [Mt/year]**

	The annual saving of CO2-equivalent emissions quantifies the reduction of GHG emissions obtained by installing a solar-based renewable energy power plant such as CSP or hybrid CSP+PV instead of a conventional fossil-fuel-based plant.
29	**Specific Land Use (SLU) [m^2/MWhe]** The specific land use is another important environmental KPI that quantifies the land required per annual electricity produced by the CSP or the hybrid CSP+PV plants.
Mixed	
30	**Levelized Cost of Electricity ($LCOE$) [EUR/MWh]** The levelized cost of energy (LCOE) is a measure of cost per unit of electricity produced over the course of the lifetime of the plant.
31	**Net Present Value (NPV) [MEUR]** The NPV is the sum of the discounted cash flows over the lifetime of the project. This KPI is defined to compare different CSP layouts or hybrid CSP+PV configurations with the state-of-the-art tower CSP plant and investigate their profitability.
32	**Discounted Pay-Back period (DPB) [years]** The discounted payback period (DPB) is the number of years necessary to recover the project cost of an investment while accounting for the time value of money.

4.1. Technical

4.1.1. Annual average Solar-to-electricity efficiency (η_{ste})

The solar-to-electric efficiency measures the ability of the power plant to transform the primary solar resource into electricity. This KPI can be calculated as the ratio between the total electric power produced in a year and the sum of the product of the irradiance (DNI_i) and the heliostat field area (A_{SF}) as shown in Equation (156).

$$\eta_{ste} = \frac{\sum_{i=1}^{8760} W_{net_i}\,[W]}{\sum_{i=1}^{8760} DNI_i\left[\frac{W}{m^2}\right]\cdot A_{SF}[m^2]}\cdot 100\ [\%] \qquad (156)$$

where W_{net_i} is the power block net electric output at each time step.

4.1.2. Annual average Receiver efficiency (η_{rec})

The receiver efficiency measures the ability of the receiver to convert the solar resource concentrated on the receiver into output thermal power. This KPI can be calculated as the ratio between the total output receiver power (Q_{rec}) and the sum of the total input receiver power as shown in Equation (157).

$$\eta_{ste} = \frac{\sum_{i=1}^{8760} Q_{rec_i}\,[W]}{\sum_{i=1}^{8760} DNI_i\left[\frac{W}{m^2}\right]\cdot A_{SF}[m^2]\cdot \eta_{opt,SF_i}\,[-]}\cdot 100\ [\%] \qquad (157)$$

where DNI_i is the irradiance at the design point, A_{SF} is the heliostat field area, and η_{opt,SF_i} is the optical efficiency of the solar field.

4.1.3. Power Block design efficiency (η_{PB})

The power block efficiency measures the ability of the power block to convert thermal power into electric power. This KPI can be calculated at the design point as the ratio between the gross output electric power ($P_{gross,des}$) and the input thermal power as shown in Equation (158).

$$\eta_{PB} = \frac{P_{gross}\,[MW]}{Q_{heater}[MW]} \cdot 100\ [\%] \tag{158}$$

4.1.4. Power Block Off-design efficiency ($\eta_{PB,off}$)

The power block off-design efficiency measures the ability of the power block to convert thermal power into electric power during off-design conditions. This KPI is provided as three efficiency values calculated for operating powers equal to 25%, 50%, and 75% of the design power. The calculations for these three efficiency values are provided in Equation (159), (160), and (161).

$$\eta_{PB_{25\%}} = \frac{P_{gross_{25\%}}\,[MW]}{Q_{heater_{25\%}}[MW]} \cdot 100\ [\%] \tag{159}$$

$$\eta_{PB_{50\%}} = \frac{P_{gross_{50\%}}\,[MW]}{Q_{heater_{50\%}}[MW]} \cdot 100\ [\%] \tag{160}$$

$$\eta_{PB_{75\%}} = \frac{P_{gross_{75\%}}\,[MW]}{Q_{heater_{75\%}}[MW]} \cdot 100\ [\%] \tag{161}$$

4.1.5. Storage efficiency (η_{TES})

The Thermal Energy Storage (TES) efficiency measures the ability of the storage to store the thermal energy over a specified period. It is defined as the ratio of energy available to energy charged in the storage. The energy available is estimated as the sum over a year of the thermal power sent to the power block ($Q_{in,PB}$). On the other side, the energy charged in the storage is estimated as the sum of the thermal power coming from the receiver or an indirect heat exchanger to the storage ($Q_{in,TES}$). Equation (162) shows the calculation of this KPI.

$$\eta_{TES} = \frac{\sum_{i=1}^{8760} Q_{in,PB_i}}{\sum_{i=1}^{8760} Q_{in,TES_i}} \cdot 100\ [\%] \tag{162}$$

4.1.6. Capacity Factor (CF)

The Capacity Factor is a measure of how much energy is produced by a plant compared to its maximum output based on the installed capacity. It is calculated by dividing the total energy produced in a year by the amount of energy it would have produced if it ran at full output over that year. In formula:

$$CF = \frac{\sum_{i=1}^{8760} W_{net_i}}{P_{name} \cdot 8760} \cdot 100\ [\%] \tag{163}$$

where W_{net_i} is the net electric output produce at each time step by the plant and P_{name} is the nominal installed capacity (power block, PV, and BESS).

4.1.7. Hybrid Capacity Factor (HCF)

The Hybrid Capacity Factor is a measure of how much energy is produced by a plant compared to its maximum output based on the load to fulfill. It is calculated by dividing the maximum energy could be injected to the grid over that year. In formula:

$$HCF = \frac{\sum_{i=1}^{8760} W_{net_i}}{\sum_{i=1}^{8760} W_{load_i}} \cdot 100 \ [\%] \quad (164)$$

where W_{net_i} is the net electric output produce at each time step by the plant and W_{load_i} is the maximum power that can be injected to the grid at each time step.

4.1.8. Availability Factor (AF)

The availability factor is a measure of the availability of a power plant indicating the fraction of time that it can produce electricity over a certain period. To analyse plant availability performance, generation unit outages should be scrutinized to identify the causes of unplanned or forced energy losses and to reduce the planned energy losses. Reducing outages increases the number of operating hours, therefore increases the plant availability factor [25]. The Availability Factor of the power plant can be calculated using Equation (165).

$$AF = \frac{\sum_{i=1}^{8760} i \ when \ W_{net_i} > 0}{8760} \cdot 100 \ [\%] \quad (165)$$

where W_{net_i} is the power block net electric output at each time step.

4.1.9. Capacity Value (CV)

The Capacity Value measures the contribution of a power plant to reliably meeting demand [26]. The capacity value is the contribution that a plant makes toward the planning reserve margin and it is expressed in terms of physical capacity (MW). Thus a plant with a nameplate capacity of 150 MW could have a capacity value of 75 MW. It is defined using the weighted Loss-of-Load-Probability (LOLP) approximation method. This method is based on the capacity factor of the CSP plant during the highest-load hours. The capacity factors are weighted, however, based on the hourly LOLPs. This weighting is done since the capacity provided by the CSP is especially needed during hours with higher LOLPs. The weights (w_i) are obtained using Equation (166).

$$w_i = \frac{LOLP_i}{\sum_{j=1}^{8760} LOLP_j} \ [-] \quad (166)$$

where $LOLP_i$ is the loss-of-load-probability calculated at each time step as the probability of available generating capacity (G_i) being less than the demand (L_i). This can be expressed as:

$$LOLP_i = P(G_i < L_i \,) \ [-] \quad (167)$$

These weights are then used to calculate the weighted average capacity factor of the CSP plant in the highest-load hours as:

$$CV = \sum_{i=1}^{8760} w_i \cdot CF_i \cdot P_{gross} \ [MW] \quad (168)$$

where CF_i is the capacity factor of the CSP plant during the *i*-th hour.

4.1.10. Heat Transfer Fluid (HTF) Maximum Temperature ($T_{max,HTF}$)

The Heat Transfer Fluid (HTF) maximum temperature is the maximum temperature of the working fluid flowing into the receiver. It's a measure of the highest quality thermal power available in the plant and it can be used to compare different layouts of the CSP plant. Higher the maximum HTF temperature, the higher the potential solar-to-electric efficiency. Equation (169) shows its formulation.

$$T_{max,HTF} = \max(T_{HTF}) \ \ [°C] \quad (169)$$

4.1.11. Heat Transfer Fluid (HTF) Temperature Difference (ΔT_{HTF})

The Heat Transfer Fluid (HTF) temperature difference coupled with the $T_{max,HTF}$ characterizes the receiver temperature design conditions and it is a measure of how compact the receiver can be. For a fixed solar field size, the maximum allowable flux that the receiver material can withstand is a function of the HTF characteristics, receiver material, receiver area and operating temperature. For example, by increasing the receiver temperatures, the receiver dimensions need to increase as well to preserve the maximum allowable flux. Equation (170) shows its formulation.

$$\Delta T_{HTF} = T_{max,HTF} - T_{min,HTF}\ [°C] \tag{170}$$

4.1.12. Storage Utilisation Factor (UF_{TES})

The storage utilisation factor (UF_{TES}) is an indicator that identifies whether the storage size used for a particular configuration is too big or too small in terms of capacity [27]. It can be defined as the ratio between total thermal energy stored and the maximum energy that could have been stored if the storage was completely emptied and filled every day.
The storage utilisation factor is calculated with Equation (171).

$$UF_{TES} = \frac{\sum_{i=1}^{8760} Q_{in,TES_i}}{E_{TES}\ [MWh] \cdot 365} \cdot 100\ [\%] \tag{171}$$

where Q_{in,TES_i} is the thermal power coming from the receiver or an indirect heat exchanger and injected into the storage at every time step, and E_{TES} is the storage capacity. Under this definition, a utilization factor of 100% means that the storage is filled every day, possibly limiting electricity production. In that case, larger storage should be investigated. Conversely, lower utilisation values indicate the storage might be oversized when compared to the rest of the system.

4.1.13. Annual Energy Yield (AEY)

The annual energy yield provides the total annual electricity generation of the power plant. Considering a hybrid CSP+PV system, the EPY is calculated as the sum of the net electrical power generated by the power block ($W_{net_{CSP_i}}$) and the net power injected into the grid by the PV field $W_{net_{PV_i}}$ over one year as shown in Equation (172).

$$AEY = \sum_{i=1}^{8760} W_{net_{CSP_i}} + W_{net_{PV_i}} + W_{netBESS_i} [MWh] \tag{172}$$

4.1.14. PV-direct-share of Electricity Produced per Year ($f_{PV,AEY}$)

The PV-share of AEY is a KPI that quantifies how much the PV-field impacts on the total electricity production of a hybrid PV+CSP plant. It is defined as the share between the sum of the PV net power injected into the grid $W_{net_{PV_i}}$ over the AEY as defined in Equation (173).

$$f_{PV,AEY} = \frac{\sum_{i=1}^{8760} W_{net_{PV_i}}}{AEY} \cdot 100\ [\%] \tag{173}$$

4.1.15. Power Block Ramping Capability (RC_{PB})

The ramping capability provides an estimate of how well the power block can adjust its power output to changing load requirements or market conditions [28]. Upward and downward ramping should be assessed separately. The ramp rate is established to prevent undesirable effects due to rapid changes in loading or discharge. The Ramping Capability is defined as the rate of change in instantaneous output from the power block. This KPI can be estimated by calculating the maximum change in power output between any 2 hours over the observation period (e.g. one year) [29]. The hours immediately before start-up and shut down are eliminated from the analysis. The Ramping Capability (Upwards) (RC_{UP}) can be calculated using Equation (174).

$$RC_{UP} = max_{i=2:n}(P_i - P_{i-1}) \left[\frac{MW}{h}\right] \tag{174}$$

where P_i is the power output [MW] at the i-th time step, while P_{i-1} is the power output at the previous time step. Similarly, the Ramping Capability (Downwards) (RC_{UP}) can be calculated using Equation (175).

$$RC_{DW} = max_{i=2:n}(P_{i-1} - P_i)\left[\frac{MW}{h}\right] \tag{175}$$

4.1.16. Power Block Block Start-up Duration (SUD_{PB})

The start-up duration is a measure of the period needed by the power block to reach the desired power output from off mode. The start-up time depends strongly on the type of the power plant. Three start-up conditions can be identified: hot, warm and cold start-ups. The start-up duration depends on the stand-still time which is less than 12 h for hot start-up from 12 to 48 h for warm and more than 48 h for cold start-up [28]. The start-up duration (SUD_{PB}) can be calculated accordingly to Equation (176).

$$SUD_{PB} = |t_1 - t_2|[hours] \tag{176}$$

where t_1 is the time when the decision was made that the generator should reach the desired power output, and t_2 is the time when the desired power output has been reached.

4.1.17. Power Block Block Shut-down Duration (SDD_{PB})

The shut-down duration is a measure of the period needed by the power block to reach the off mode from the operating power output condition. The shut-down duration (SDD_{PB}) can be calculated accordingly to Equation (177).

$$SDD_{PB} = |t_1 - t_2|[hours] \tag{177}$$

where t_1 is the time when the decision was made that the generator should be switched-off, and t_2 is the time when the desired power output has been reached.

4.1.18. Flexibility Factor (FF)

The flexibility factor indicates the ability to shift energy production from low to high price periods. If the energy production is similar in low and high price periods, the factor is 0. If electricity is produced only in high price periods, the factor is 1. This KPI can be defined as:

$$FF = \frac{\int_0^{l(high-price)} W_{net}dt - \int_0^{l(low-price)} W_{net}dt}{\int_0^{l(high-price)} W_{net}dt + \int_0^{l(low-price)} W_{net}dt}[-] \tag{178}$$

The flexibility factor varies between −1 and 1 whereas −1 correlates to a highly inflexible controlled system and 1 indicates the highest desired flexibility. One of the limitations of this factor is that other grid signals or climatic conditions will lead to different values of flexibility factor [30], [31].

4.2. Economic

4.2.1. Capital Expenditure ($CAPEX$)

The investment costs or capital expenditure ($CAPEX$) accounts for all the investment incurred along with the development of the project, including direct and indirect costs. Direct costs refer mainly to all costs in connection to the purchase and installation of the equipment (e.g. receiver, power block components, thermal energy storage etc.), whereas indirect costs refer to all remaining costs incurred, for instance in connection to engineering, procurement and contingency during project development [32]. The CAPEX definition is available in Section 3.2 for CSP, PV, and BESS.

4.2.2. PV-share of CAPEX ($f_{PV,CAPEX}$)

The PV-share of CAPEX is a KPI that quantifies how much the PV-field impacts on the total investment cost of a hybrid PV+CSP plant. It is defined as the share between the PV direct costs over the system direct costs as defined in Equation (179).

$$f_{PV,CAPEX} = \frac{C_{direct,PV}}{CAPEX_{direct}} \cdot 100\ [\%] \tag{179}$$

4.2.3. Operational Expenditure ($OPEX$)

The OPEX relates to the operational and maintenance costs incurred during the operation of the power plant. These include fixed cost and production-dependent cost as shown in Equation (180). The annual fixed cost (C_{year}) and the specific operating and maintenance costs factor ($OM_{production}$) are assumed based on the specific layout under investigation. Then, the production-dependent costs are obtained as the product between $OM_{production}$ and the electricity produced per year (EPY).

$$OPEX = C_{year}\left[\frac{EUR}{year}\right] + OM_{production}\left[\frac{EUR}{MWh}\right] \cdot EPY\left[\frac{MWh}{year}\right]\ \left[\frac{EUR}{year}\right] \tag{180}$$

For specific layouts involving fossil-fuel burner or integration with the grid, the corresponding costs will be added to the definition provided above.

4.2.4. Specific CAPEX (S_{CAPEX})

The specific CAPEX is the investment cost per unit of installed capacity and it can be defined as the ratio between the CAPEX and the nameplate capacity (P_{name}) as shown in Equation (181).

$$S_{CAPEX} = \frac{CAPEX}{P_{name}}\ \left[\frac{EUR}{MW}\right] \tag{181}$$

This KPI can be used to compare large-scale and small-scale configurations based on their investment cost. Considering the same layout, varying the scale, this KPI can reveal how the scale influences economic profitability.

4.2.5. Specific Cost of Thermal Energy Storage (SC_{TES})

The specific cost of the thermal energy storage quantifies the cost required to store a unit of thermal energy at the desired temperature and with the specific storage media selected. It is calculated as the ratio between the cost of the storage (C_{TES}) divided by the storage capacity (E_{TES}), as shown in Equation (182).

$$SC_{TES} = \frac{C_{TES}}{E_{TES}}\ \left[\frac{EUR}{MWh}\right] \tag{182}$$

This KPI can be used to compare and benchmark different storage options for the CSP-only or hybrid configurations under investigation.

4.2.6. Specific cost of the Heat Transfer Fluid (HTF) system (SC_{HTF})

The specific cost of the Heat Transfer Fluid (HTF) system quantifies the cost of a unit of thermal energy converted from solar irradiation in the receiver, exchanged in intermediate heat exchangers (if any), and to be stored. The total cost of the HTF system is estimated as the sum of the cost of the receiver (C_{rec}), the cost of the circulators (C_{pumps}), and the cost of the heat exchangers (C_{HX}) included if an indirect storage system is adopted. Then, the specific cost of the HTF system is calculated by dividing the total cost by the receiver design power ($Q_{rec,des}$) as shown in Equation (183).

$$SC_{HTF} = \frac{C_{rec} + C_{pumps} + C_{HX}}{Q_{rec,des}}\ \left[\frac{EUR}{kW}\right] \tag{183}$$

This KPI can be used to compare and benchmark different HTF options, direct versus indirect storage options for the CSP-only plant. If a hybrid configuration is under investigation, the electric heater and the corresponding circulators will become part of the costs.

4.2.7. Share of the cost of the conventional components ($f_{soa,CAPEX}$)

The share of the cost of the conventional components quantifies the impact of conventional components on the total investment cost of a solar-based renewable energy plant. This KPI is also a measure of what drives the CAPEX the most. Thus, low $f_{soa,CAPEX}$ values mean that the CAPEX is mainly driven up by innovative components. Equation (184) shows the definition of this KPI as the share between the conventional components over the system direct costs.

$$f_{soa,CAPEX} = \frac{C_{conventional}}{CAPEX_{direct}} \cdot 100\ [\%] \qquad (184)$$

where $C_{conventional}$ is the sum of the costs of conventional components installed in the layout under investigation. The components are identified based on the specific study case.

4.2.8. Specific Cost of Power Block (SC_{PB})

The specific cost of the power block quantifies the cost of a unit of installed electric power capacity. It is calculated as the ratio between the cost of the power block (C_{PB}) divided by the installed capacity (P_{gross}), as shown in Equation (185).

$$SC_{PB} = \frac{C_{PB}}{P_{gross}} \left[\frac{EUR}{kW}\right] \qquad (185)$$

This KPI can be used to compare and benchmark different power block configurations for the layout under investigation.

4.3. Environmental

4.3.1. Specific Water Consumption (SWC)

Although CSP technology is a sustainable source of energy, a relatively high water consumption is necessary to keep the system in good operation [33]. For examples, case studies located in Egypt, Libya, Morocco and Tunisia showed that solar tower CSP plants with wet cooling require up to 2200 m^3/GWh of total water demand [34]. By employing a dry cooling or a hybrid cooling concept it is possible to reduce the overall water consumption for a CSP. The average water demand for solar tower CSP plants can be reduced to 340 m^3/GWh [34].
Furthermore, in arid regions where CSP technology has typically a high potential due to favourable irradiation, high soiling rates can occur due to the combination of low precipitation and dusty conditions. The dust and sand accumulate on the mirrors, which results in the light being scattered and absorbed leading to a reduction in reflectance as a result [35]. For this reason, regular cleaning of the CSP mirror surfaces and PV module surfaces is required, which needs a considerable amount of water making soiling an important factor for the overall water consumption of a CSP and CSP-PV hybrid plant.
The total water demand of the CSP or hybrid CSP+PV plant is estimated as the sum of the water required by the cooling system ($V_{cooling}$), by the mirrors + PV modules cleaning system ($V_{cleaning}$) plus a miscellaneous term (V_{misc}) considering service water, sanitary/sewage water etc. The Specific Water Consumption (SWC) is calculated in Equation (186) as the ratio between the total water demand and the EPY.

$$SWC = \frac{\sum_h^{8760} V_{cooling_h} + V_{cleaning_h} + V_{misc_h}\ [m^3]}{EPY\ [MWh]/1000} \left[\frac{m^3}{GWh}\right] \qquad (186)$$

4.3.2. Annual saving of $CO_{2,eq}$ emissions ($\Delta CO_{2,eq}$)

The annual saving of CO_2-equivalent emissions quantifies the reduction of GHG emissions obtained by installing a solar-based renewable energy power plant such as CSP or hybrid CSP+PV instead of a conventional fossil-fuel-based plant.
The environmental impact of fossil fuel power plants is not limited to carbon dioxide (CO_2) emissions, but rather extends to carbon monoxide (CO), nitrogen oxides (NO_x), and sulphur oxides (SO_x). The

contribution of all these gasses combined are expressed in terms of equivalent carbon dioxide emissions ($CO_{2,eq}$). The annual saving of CO2-equivalent emissions is calculated as the difference between the renewable power plant emissions and the corresponding emissions of the electricity generation mix, as shown in Equation (187).

$$\Delta CO_{2,eq} = \left| CO_{2,eq}^{plant} \left[\frac{Mt}{year}\right] - f_{CO_{2,eq}} \left[\frac{kg}{kWh}\right] \cdot EPY \left[\frac{MWh}{year}\right] \right| \left[\frac{Mt}{year}\right] \quad (187)$$

The emissions of the plant under investigation are almost negligible compared to conventional power plants except for configurations that include fossil-fuel burners or integration with the grid. According to [36], the mean life cycle GHG emissions for both PV and CSP central receiver systems are estimated to 0.085 kg/kWh. Nowadays, during the operating phase of such plants, the main source of GHG emissions is related to conventional trucks emissions employed to clean the mirrors and the PV modules.
The corresponding emissions of the electricity generation mix are estimated as the product between the grid emission factor ($f_{CO_{2,eq}}$) and the electricity produced per year estimated for the renewable energy plant.
The grid emission factor is reported in Table 30 for different macro-areas. This indicator provides the average equivalent kilograms of CO_2 emitted by the generation mix per unit of electricity injected in a specific geographic area [37].

Table 30. Grid emission factor for different macro-areas

Area	$f_{CO_{2eq}}$ $[kg_{CO_{2eq}}/kWh]$	Reference
Europe	0.339	[38]
North and Central America	0.357	[39], [40], [41]
South America	0.226	[40]
Asia	0.655	[40], [42]
Australasia	0.451	[43], [44]
Middle East	0.565	[40], [45]
Africa	0.961	[40]

The countries considered for each specific area and their grid emission factors are reported in Appendix A.

4.3.3. Specific Land Use (SLU)

The specific land use is another important environmental KPI that quantifies the land required per annual electricity produced by the CSP or the hybrid CSP+PV plants. This KPI allows performing comparisons between different layouts and can be fundamental to drive decisions on which layout prioritize in highly-populated areas like in Europe. It can be calculated as the ratio between the total area occupied by the plant (A_{land}) and the sum over the year of the net electric power produced (W_{net}), as shown in Equation (188).

$$SLU = \frac{A_{land}}{\sum_{i=1}^{8760} W_{net_i}} \left[\frac{m^2}{MWh}\right] \quad (188)$$

Solar power plants are likely to affect significantly more land than other electricity sources due to their low power density. The average total land-use requirements are 14.6 m^2/MWh/yr for PV and 14.2 m^2/MWh/yr for CSP for several solar power plants analysed in [46]. Solar land use depends on specific technology choices, such as cell efficiency, tracking method, the inclusion of thermal energy storage, and are a function of the solar resource available at each site.

4.4. Mixed

4.4.1. Levelized Cost of Electricity ($LCOE$)

The levelized cost of energy (LCOE) is a measure of cost per unit of electricity produced over the course of the lifetime of the plant. LCOE has the advantage of compressing all the direct technology costs into a single metric which is easy to understand and allows to compare alternative technologies with different scales of operation, different investment and operating periods, [47]. The LCOE can be calculated as presented in Equation (189) considering the total capital expenditure (CAPEX), the annual operating expenditure (OPEX), and the Annual Energy Yield (AEY) [48].

$$LCOE = \frac{(CAPEX\ [EUR] \cdot CRF)\ \left[\frac{EUR}{year}\right] + OPEX\ \left[\frac{EUR}{year}\right]}{AEY\ \left[\frac{MWh}{year}\right]} \left[\frac{EUR}{MWh}\right] \quad (189)$$

where CRF is the Capital Recovery Factor, defined in Equation (190), as a function of the real discount rate (r) and of the lifetime of the plant (N):

$$CRF = \frac{r(1+r)^N}{(1+r)^N - 1} \quad (190)$$

The real discount rate is calculated as presented in Equation (191) as a function of the nominal discount rate (d) and of the interest rate (i).

$$r = \frac{(1+r)}{(1+i)} - 1 \quad (191)$$

4.4.2. Net Present Value (NPV)

The Net Present Value is defined to compare different CSP layouts or hybrid CSP+PV configurations with the state-of-the-art tower CSP plant and investigate their profitability. This KPI allows for a clear comparison with different investment options by examining costs (cash outflows) and revenues (cash inflows) together [47]. The NPV is calculated with Equation (192), where FCF_i represents the free cash flow of the project during the i-th year of operation, N stands for the operational lifetime of the project, and r refers to the real discount rate.

$$NPV = -CAPEX + \sum_{i=1}^{N} \frac{FCF_i}{(1+r)^i}\ [EUR] \quad (192)$$

This FCF_i is the operational profits of the plant defined as the difference between the revenues and the operating cost as shown in Equation (193). Revenues and operating cost can be expressed as presented in Equation (194) and (195) respectively.

$$FCF_i = Revenues_i - Operating\ costs_i \quad (193)$$

$$Revenues_i = \sum_h^{8760} \lambda_h \left[\frac{EUR}{MWh}\right] \cdot W_{net_h}[MWh] \quad (194)$$

$$Operating\ costs_i = OPEX_i \left[\frac{EUR}{year}\right] \quad (195)$$

where λ_h and $W_{net,h}$ are the electricity price and electricity sold in the hour h, respectively.

4.4.3. Discounted Payback Period (DPB)

The discounted payback period (DPB) is the number of years necessary to recover the project cost of an investment while accounting for the time value of money. DPB is recommended when risk is an issue (i.e., significant uncertainties are present) because DPB allows for a quick assessment of the duration during which an investor's capital is at risk [47]. Equation (196) shows how to calculate the discounted payback period for a constant free cash flow.

$$DPB = \frac{\ln FCF - \ln(FCF - r \cdot CAPEX)}{\ln(1 + r)} \quad (196)$$

5. Conclusion

In this work, an upscaled layout for the Powder2Power project has been defined, along with the techno-economic modeling approach, including thermodynamic models and bottom-up cost functions. The project's key performance indicators (KPIs) panel has also been established to evaluate the benefits of Powder2Power in simulation activities.

MoSES, the techno-economic modeling tool introduced in Task 5.3, plays a central role in supporting the evaluation of Powder2Power benefits. It offers capabilities for designing, optimizing, and benchmarking various solar plant layouts. The modeling approach developed focuses on system design, cost structures, and expected performance, providing a solid foundation for further analysis.

The KPI panel, integrated into the tool, allows for a comprehensive assessment of technical, economic, environmental, and mixed performance indicators. This integration enables users to select specific KPIs as objective functions for system optimization, enhancing the flexibility and applicability of the tool.

Future activities will continue in Task 5.3, focusing on further development and verification of the techno-economic model. This includes incorporating inputs from other partners on modeling case studies and layout definitions, as well as integrating feedback from industrial partners into the cost functions and model assumptions.

Reference list

[1] S. Guccione and R. Guedez, “Moses – the New Techno-Economic Optimization Modeling Tool for Hybrid Solar Power Plants,” in *Proceedings of Solar World Congress 2023*, Freiburg, Germany: International Solar Energy Society, 2023, pp. 1–9. doi: 10.18086/swc.2023.08.02.

[2] S. Guccione and R. Guedez, “Techno-economic optimization of molten salt based CSP plants through integration of supercritical CO2 cycles and hybridization with PV and electric heaters,” *Energy*, vol. 283, p. 128528, 2023, doi: https://doi.org/10.1016/j.energy.2023.128528.

[3] I. H. Bell, J. Wronski, S. Quoilin, and V. Lemort, “Pure and pseudo-pure fluid thermophysical property evaluation and the open-source thermophysical property library coolprop,” *Ind Eng Chem Res*, vol. 53, no. 6, pp. 2498–2508, 2014, doi: 10.1021/ie4033999.

[4] P. Gilman *et al.*, “PySAM (Python Wrapper for System Advisor Model ‘SAM’),” 2019, *USDOE Office of Energy Efficiency and Renewable Energy (EERE). Renewable Power Office. Solar Energy Technologies Office, Web*. doi: 10.11578/dc.20190903.1.

[5] K. J.F., W. K., N. C.L., and S. M.J, “Genetic Algorithms and Their Application to In Silico Evolution of Genetic Regulatory Networks,” in *Computational Biology. Methods in Molecular Biology (Methods and Protocols), vol 673*, Totowa, NJ.: Humana Press, 2010. doi: https://doi.org/10.1007/978-1-60761-842-3_19.

[6] J. Blank and K. Deb, “Pymoo: Multi-Objective Optimization in Python,” *IEEE Access*, vol. 8, pp. 89497–89509, 2020, doi: 10.1109/ACCESS.2020.2990567.

[7] K. Deb and J. Sundar, “Reference point based multi-objective optimization using evolutionary algorithms,” *GECCO 2006 - Genetic and Evolutionary Computation Conference*, vol. 1, pp. 635–642, 2006, doi: 10.1145/1143997.1144112.

[8] M. L. Bynum *et al.*, *Pyomo - Optimization Modeling in Python*, 3rd ed. Springer, 2021.

[9] NOAA Global Monitoring Division, “General Solar Position Calculations,” 2015.

[10] L. F. González-portillo, K. Albrecht, and C. K. Ho, “Techno-Economic Optimization of CSP Plants with Free-Falling Particle Receivers,” 2021, doi: 10.3390/e23010076.

[11] L. F. González-Portillo, K. Albrecht, and C. K. Ho, “Techno-economic optimization of CSP plants with free-falling particle receivers,” *Entropy*, vol. 23, no. 1, pp. 1–24, Jan. 2021, doi: 10.3390/e23010076.

[12] B. Mills, R. Shaeffer, C. K. Ho, and L. Yue, “Modeling the Thermal Performance of Falling Particle Receivers Subject to External Wind,” in *The 13th International Conference on Energy Sustainability*, Bellevue, WA, Jul. 2019.

[13] C. K. Ho, B. Mills, and J. M. Christian, “VOLUMETRIC PARTICLE RECEIVERS FOR INCREASED LIGHT TRAPPING AND HEATING,” 2016. [Online]. Available: www.unifrax.com

[14] C. K. Ho *et al.*, “Characterization of particle flow in a free-falling solar particle receiver,” *Journal of Solar Energy Engineering, Transactions of the ASME*, vol. 139, no. 2, Apr. 2017, doi: 10.1115/1.4035258.

[15] L. F. González-Portillo, R. Abbas, K. Albrecht, and C. Ho, “Analysis of optical properties in particle curtains,” *Solar Energy*, vol. 213, pp. 211–224, Jan. 2021, doi: 10.1016/j.solener.2020.11.012.

[16] B. Gobereit, L. Amsbeck, R. Buck, R. Pitz-Paal, M. Röger, and H. Müller-Steinhagen, “Assessment of a falling solid particle receiver with numerical simulation,” *Solar Energy*, vol. 115, pp. 505–517, May 2015, doi: 10.1016/j.solener.2015.03.013.

[17] European Central Bank, “Euro foreign exchange reference rates: average 2021 US dollar excahnge rate.” [Online]. Available: https://www.ecb.europa.eu/ stats/

policy_and_exchange_rates/ euro_reference_exchange_rates/ html/ eurofxref-graph-usd.en.html

[18] USA DoE, "Gen 3 CSP Topic 1–Phase 3 Test Facility Down-Selection Criteria," 2019, *Washington, DC, USA*.

[19] T. Bauer *et al.*, "Blueprint for molten salt CSP power plant. Final report of the project: CSP-Reference Poweer Plant," p. 158, 2021.

[20] C. S. Turchi *et al.*, "CSP Systems Analysis - Final Project," *Nrel/TP-5500-72856*, no. May, 2019.

[21] C. K. Ho, M. Carlson, P. Garg, and P. Kumar, "Cost and Performance Tradeoffs of Alternative Solar-Driven s-CO2 Brayton Cycle Configurations," in *ASME 2015 9th International Conference on Energy Sustainability collocated with the ASME 2015 Power Conference*, 2015. doi: 10.1115/ES2015-49467.

[22] N. T. Weiland, B. W. Lance, and S. R. Pidaparti, "sCO2 Power Cycle Component Cost Correlations From DOE Data Spanning Multiple Scales and Applications," in *ASME Turbo Expo 2019: Turbomachinery Technical Conference and Exposition*, 2019, pp. 1–17. doi: 10.1115/GT2019-90493.

[23] A. Zurita, C. Mata-Torres, J. M. Cardemil, R. Guédez, and R. A. Escobar, "Multi-objective optimal design of solar power plants with storage systems according to dispatch strategy," *Energy*, vol. 237, 2021, doi: 10.1016/j.energy.2021.121627.

[24] R. Fu, D. J. Feldman, and R. M. Margolis, "U.S. Solar Photovoltaic System Cost Benchmark: Q1 2018," Golden, CO: National Renewable Energy Laboratory. NREL/TP-6A20-72399, 2018. doi: 10.2172/1483475.

[25] Public Utilities Commission of Sri Lanka;, "Performance Measurements of Generation and Transmission Systems," 2014, *Public Utilities Commission of Sri Lanka*.

[26] S. H. Madaeni, R. Sioshansi, and P. Denholm, "Capacity value of concentrating solar power plants," *Concentrating Solar Power: Data and Directions for an Emerging Solar Technology*, no. June, pp. 149–186, 2012.

[27] J. Garcia, R. Guedez, V. Smet, and A. Sorce, "Techno-economic optimization of a combined cycle combined heat and power plant with integrated heat pump and low-temperature thermal energy storage," *Proceedings of the ASME Turbo Expo*, vol. 5, pp. 1–12, 2020, doi: 10.1115/GT2020-16072.

[28] Magnitude - European Founded Project (GA: 774309), "Deliverable 6.1 - KPIs and assessment procedure," 2019.

[29] B. Kirby and M. Milligan, "A Method and Case Study for Estimating the Ramping Capability of a Control Area or Balancing Authority and Implications for Moderate or High Wind Penetration," *Proceedings of the WindPower 2005*, pp. 1–16, 2005.

[30] C. Finck, R. Li, R. Kramer, and W. Zeiler, "Quantifying demand flexibility of power-to-heat and thermal energy storage in the control of building heating systems," *Appl Energy*, vol. 209, no. July 2017, pp. 409–425, 2018, doi: 10.1016/j.apenergy.2017.11.036.

[31] J. Le Dréau and P. Heiselberg, "Energy flexibility of residential buildings using short term heat storage in the thermal mass," *Energy*, vol. 111, pp. 991–1002, 2016, doi: 10.1016/j.energy.2016.05.076.

[32] R. Guédez, *A Techno-Economic Framework for the Analysis of Concentrating Solar Power Plants with Storage*. 2016.

[33] L. Haack and M. Schlecht, "Water saving potential of CSP-PV hybrid plants," *AIP Conf Proc*, vol. 2126, no. July, 2019, doi: 10.1063/1.5117762.

[34] K. Damerau, K. Williges, A. G. Patt, and P. Gauché, "Costs of reducing water use of concentrating solar power to sustainable levels: Scenarios for North Africa," *Energy Policy*, vol. 39, no. 7, pp. 4391–4398, 2011, doi: 10.1016/j.enpol.2011.04.059.

[35] S. Bouaddi and A. Ihlal, “Monthly soiling comparison of CSP candidate mirrors exposed in southwest Morocco,” *Mater Today Proc*, vol. 3, no. 7, pp. 2556–2561, 2016, doi: 10.1016/j.matpr.2016.04.002.

[36] R. Kommalapati, A. Kadiyala, M. T. Shahriar, and Z. Huque, “Review of the life cycle greenhouse gas emissions from different photovoltaic and concentrating solar power electricity generation systems,” *Energies (Basel)*, vol. 10, no. 3, 2017, doi: 10.3390/en10030350.

[37] Carbon Footprint, “Carbon Footprint, Country specific Electricity Factors,” no. June, pp. 1–10, 2019.

[38] Association of Issuing Bodies (AIB), “2018 Residual Mix Factors,” 209AD.

[39] Environment and Climate Change Canada, *National inventory report 1990-2017: GHG sources and sinks in Canada (Part 3)*. 2019.

[40] P. Eigen and A. Umana, “The G20 Transition to a Low-Carbon Economy,” 2018.

[41] EPA United States Environmental Protection Agency, “Emissions & Generation Resource Integrated Database (eGRID).” [Online]. Available: https://www.epa.gov/energy/emissions-generation-resource-integrated-database-egrid

[42] HK Electric Investments, “Greener Power Going Further - Sustainability Report 2018,” 2018.

[43] Australian National Greenhouse Accounts - Department of the Environment and Energy, “National Greenhouse Accounts Factors,” 2017.

[44] New Zealand Government, “Measuring Emissions: A Guide for Organisations - 2020 Summary of Emission Factors,” 2020.

[45] K. InternationalAG, “Sustainability report 2019,” *Global reporting initiative (GRI)*, no. 2019, pp. 0–141, 2019.

[46] Sean Ong, C. Campbell, P. Denholm, R. Margolis, and G. Heath, “Land-Use Requirements for Solar Power Plants in the United States,” 2006. doi: 10.1016/j.rapm.2006.08.004.

[47] W. Short, D. Packey, and T. Holt, “A manual for the economic evaluation of energy efficiency and renewable energy technologies,” *Renew Energy*, vol. 95, no. March, pp. 73–81, 1995, doi: NREL/TP-462-5173.

[48] L. F. González-portillo, K. Albrecht, and C. K. Ho, “Techno-Economic Optimization of CSP Plants with Free-Falling Particle Receivers,” 2021.

[49] Climate Transparency, “Brown to Green - The G20 Transition to a low-carbon economy,” 2018. [Online]. Available: http://www.climate-transparency.org/g20-climate-performance/g20report2018

Appendix A. Grid emission factor for different countries

Table 31. Grid emission factor for different countries in Europe

Area	$f_{CO_{2eq}}\ [kg_{CO_{2eq}}/kWh]$	Reference
Austria	0.142	[38]
Belgium	0.167	[38]
Bulgaria	0.470	[38]
Croatia	0.417	[38]
Cyprus	0.639	[38]
Czech Republic	0.576	[38]
Denmark	0.209	[38]
Estonia	0.875	[38]
Finland	0.143	[38]
France	0.047	[38]
Germany	0.469	[38]
Greece	0.567	[38]
Hungary	0.314	[38]
Iceland	0.000	[38]
Ireland	0.393	[38]
Italy	0.327	[38]
Latvia	0.313	[38]
Lithuania	0.362	[38]
Luxembourg	0.201	[38]
Malta	0.761	[38]
Netherlands	0.457	[38]
Norway	0.011	[38]
Poland	0.846	[38]
Portugal	0.307	[38]
Romania	0.401	[38]
Russian Federation	0.330	[49]
Slovakia	0.169	[38]
Slovenia	0.335	[38]
Spain	0.288	[38]
Sweden	0.012	[38]
Switzerland	0.014	[38]
United Kingdom	0.237	[49]
Average	**0.339**	[38]

Table 32. Grid emission factor for different countries in North and Central America

Area	$f_{CO_{2eq}}\ [kg_{CO_{2eq}}/kWh]$	Reference
Canada	0.130	[39]
Mexico	0.464	[40]
United States	0.476	[41]
Average	**0.357**	[39], [40], [41]

Table 33. Grid emission factor for different countries in South America

Area	$f_{CO_{2eq}}\ [kg_{CO_{2eq}}/kWh]$	Reference
Argentina	0.358	[40]
Brazil	0.093	[40]

Average	**0.226**	[40]

Table 34. Grid emission factor for different countries in Asia

Area	$f_{CO_{2eq}}$ $[kg_{CO_{2eq}}/kWh]$	Reference
China (PR)	0.6236	[40]
Hong Kong (China)	0.8	[42]
India	0.7429	[40]
Indonesia	0.7551	[40]
Japan	0.4916	[40]
Korea (Republic)	0.517	[40]
Average	**0.655**	[40], [42]

Table 35. Grid emission factor for different countries in Australasia

Area	$f_{CO_{2eq}}$ $[kg_{CO_{2eq}}/kWh]$	Reference
Australia	0.800	[43]
New Zealand	0.101	[44]
Average	**0.451**	[43], [44]

Table 36. Grid emission factor for different countries in the Middle East

Area	$f_{CO_{2eq}}$ $[kg_{CO_{2eq}}/kWh]$	Reference
Saudi Arabia	0.718	[40]
Turkey	0.543	[40]
United Arab Emirates	0.433	[45]
Average	**0.565**	[40], [45]

Table 37. Grid emission factor for different countries in Africa

Area	$f_{CO_{2eq}}$ $[kg_{CO_{2eq}}/kWh]$	Reference
South Africa	0.961	[40]
Average	**0.961**	[40]